Geomorphology 445 (2024) 108971

Contents lists available at ScienceDirect

Geomorphology

journal homepage: www.journals.elsevier.com/geomorphology

A fluvial record of late Quaternary climate changes and tectonic uplift along the Marche Piedmont Zone of the Apennines: New insights from the Tesino River (Italy)

Michele Delchiaro [a], Giulia Iacobucci [a,*], Marta Della Seta [a], Natacha Gribenski [b], Daniela Piacentini [a], Valeria Ruscitto [a], Marta Zocchi [a], Francesco Troiani [a]

[a] Department of Earth Sciences, Sapienza University of Rome, P.le Aldo Moro 5, Rome, Italy
[b] Institute of Geological Sciences and Oeschger Centre for Climate Change Research, University of Bern, Baltzerstrasse 1, CH-3012, Bern, Switzerland

ARTICLE INFO

Keywords:
Fluvial fill terrace
Low-rate tectonics
Climate change
Semi-automatic terrace extraction

ABSTRACT

Fluvial terraces are a pre-eminent continental record of climate changes and tectonics. Although the use of fill terraces for incision rate derivation is complicated due to their cyclical nature relative to strath terraces, they remain a relatively complete record of incision and deposition, thus allowing one to derive interpretations about both tectonics and climate. The Adriatic piedmont of the Apennines (central Italy) offers a well-preserved staircase of such terraces, caused by the cyclical alternation of fluvial aggradation and incision over the Middle and Late Pleistocene in response to a combination of low-rate tectonic uplift and climate changes. Although the staircase has been already widely described with examples from several valleys of the Adriatic Piedmont, its geochronological constraints are limited and must be enhanced to extract reliable climatic and tectonic signals from terrace deposits—especially for the older terrace levels.

This research provides new Optically Stimulated Luminescence (OSL) data on the terrace chronology in combination with new semi-automatically extracted data on the altimetric and along-valley terrace distributions, as well as the sedimentological characteristics of fill terraces within the Tesino River basin in the Marche piedmont zone of the Apennines. The semi-automatic extraction of the terrace tread allowed a preliminary level classification as a function of the terrace height above the modern channel thalweg. The results demonstrate that, within the slowly uplifting Adriatic piedmont of the Apennines, the main phases of fluvial aggradation occurred during cold and full-glacial conditions followed by river incision and floodplain-channel abandonment during warmer periods. This finding confirms previous results from the last fluvial aggradation-incision cycle (Late Pleistocene). The results also show that the same formation mechanism is valid for the older (Middle Pleistocene) terraces. Indeed, this study provides new geochronological constraints for the regional-scale paradigm of cyclical formation and development of Quaternary fill terrace staircases along this sector of the Apennines. The use of a dated fill terrace staircase allowed estimation of a Middle Pleistocene long-term bedrock incision rate ranging from 0.3 to 0.5 mm yr^{-1} in agreement with previous studies in the central-northern sector of the Adriatic Apennines. The resulting uplift rate supports the presence of differently uplifted blocks due to the fragmentation of the peri-Adriatic region caused by the activity of left-lateral faults.

1. Introduction

Fluvial terraces are important repositories of climatically and tectonically driven changes reflected by channel aggradation and incision. The terrace stratigraphic indicators are represented by tread (or flights) (Campbell, 1929) and basal strath (Bucher, 1932) surfaces. These two constitute the flat terrace surface and its erosional terrace base, respectively. Depending on the morphology and thickness of the alluvial deposits and the dynamics of deposition, terraces can be distinguished between two end-members: i) strath (erosional) terraces characterized by a distinct sub-horizontal erosional base, commonly but not exclusively carved into bedrock, with a relatively thin alluvial cover (Merritts et al., 1994; Pazzaglia, 2013); and ii) fill (depositional) terraces presenting a thick alluvial deposit previously burying the river valley

* Corresponding author.
E-mail address: giulia.iacobucci@uniroma1.it (G. Iacobucci).

https://doi.org/10.1016/j.geomorph.2023.108971
Received 27 March 2023; Received in revised form 31 October 2023; Accepted 3 November 2023
Available online 4 November 2023

bottom (Leopold et al., 1964; Lewin and Gibbard, 2010). The bounding unconformities (tread and basal strath), if dated with geochronology or biostratigraphy, can thus become paleohydrologic chroniclers of catchment-scale climatic processes and provide timing about crustal deformation for assessing rock-uplift rates (Bull, 1991, 2007; Blum and Valastro Jr, 1994; Maddy et al., 2001).

Since the work by Penck and Brückner (1909), who examined the Danube River terraces, this dating approach has used chronological data for reconstructions in different areas from Northern Europe (Bridgland, 2000; Maddy et al., 2001; Madritsch et al., 2012; Necea et al., 2013; Stange et al., 2014) to Asia (Wang et al., 2009; Dutta et al., 2012; Hu et al., 2012; Huang et al., 2014; Gao et al., 2016; Zhang et al., 2018; Wu et al., 2020; Delchiaro et al., 2019, 2022, 2023) and South America (Viveen et al., 2022) as well as in a global perspective (Bridgland and Westaway, 2008; Mather et al., 2017). Also, there are numerous instances of works that use terraces for estimating uplift rates in tectonically active (Burbank et al., 1996; Brocard et al., 2003; Wang et al., 2004) and inactive regions (Maddy, 1997; Westaway et al., 2002; Bridgland et al., 2015).

Generally, fill (depositional) terraces are employed for research into climatic reconstructions, whereby they present a thick alluvial deposit and are not usually employed for calculating incision rates due to the cyclic nature of their formation (Schanz et al., 2018; Zondervan et al., 2022). In particular, cut-and-fill dynamics often occurs linked to different parts of a glacial-interglacial climate cycle, thus making the interpretation of these types of deposits more complex (Lewin and Gibbard, 2010). Another possible bias for the climatic and tectonic reconstructions using fill terraces is the role of lithology that can contribute to how the sedimentological signal is recorded and detected downstream. A substrate that is more able to be eroded will have greater sediment supply to the hydrological system (Bridgland, 2000; Schanz and Montgomery, 2016).

In the Marche Apennines (central Italy), well-preserved fluvial terrace staircases testify the complex interaction among tectonic uplift, climate variability, and lithological setting during the Late Quaternary. This situation has favoured the genesis and development of a staircase of three fill terraces whose treads are positioned at different heights along the valley-sides. Fill terrace formation is attributed to a timespan ranging from the Middle-Late Pleistocene to the Holocene (Lipparini, 1939; Villa, 1942; Selli, 1954, 1962; Nesci and Savelli, 1990; Coltorti et al., 1991; Della Seta et al., 2008; Wegmann and Pazzaglia, 2009). Their thickness ranges from 3 to 4 m up to 40 m (Nesci and Savelli, 1991; Fanucci et al., 1996). The fill terrace treads are positioned above the present thalweg at heights ranging from few meters (recent terraces in downstream areas) up to 130–150 m with a maximum of 200–210 m reported for the oldest terrace level of the upper Metauro valley (Nesci et al., 1990). There are unequal altimetric distributions of the same terrace level within adjacent valleys. These are usually related to tectonic differential displacements (e.g., Coltorti et al., 1996; Di Bucci et al., 2003; Della Seta et al., 2004, 2005, 2008). The formation of the terrace deposits has been ascribed to the main glacial phases of the Late Quaternary. Only the ages of the younger terrace levels (Late Pleistocene-Holocene third level) are constrained with absolute dating (see Table 1; Damiani and Moretti, 1968; Alessio et al., 1979; Coltorti, 1981; Coltorti and Nanni, 1987; Coltorti et al., 1991; Coltorti and Dramis, 1988; Nesci et al., 1995, Wegmann and Pazzaglia, 2009). The older terrace levels (second and first levels) are constrained on a morphostratigraphic basis (Wegmann and Pazzaglia, 2009). The only exception is represented by Taddeucci et al. (1992) who dated a speleothem with a $^{230}Th/^{234}U$ method obtaining an age of 160,000 ± 10,000 yr that Wegmann and Pazzaglia (2009) associated to the terrace formation (2nd level).

Cold climate-driven aggradation occurred along the glacier-free valleys within the Marche piedmont zone of the Apennines, thus highlighting the importance of climate conditions for fill terrace staircase development (Nesci et al., 2012). It is generally accepted that the upstream influence of sea-level fluctuation is conceptually limited (Schumm, 1993). Despite the proximity of the coastline to the study area, the gently sloping continental shelf extends from the north all the way to the Pescara offshore (Fig. 1, Storms et al., 2008; Cerrone et al., 2021) with no significant topographic slope break until the shelf edge is reached. Consequently, the coastline was located considerably southeast of its present position during the Last Glacial Maximum, and the drainage network extended eastward with a gentle gradient (Mayer et al., 2003). This emphasized the effect of climate relative to the mechanisms of erosion-deposition typically associated with eustacy.

Detrital sediment production caused by physical weathering (cryoclastic weathering) increases during the cold phases. Consequently, an aggrading phase begins, thus accumulating significant deposits of coarse sediment (Dramis and Bisci, 1986; Vandenberghe, 1995; Rose, 1995). In addition, the aggradation of the deposits in the study area is amplified by the lithological configuration of the area including of predominantly terrigenous sediments where the bedrock consists of Plio-Pleistocene arenitic and pelitic marine deposits covering the Late Miocene siliciclastic and evaporitic formations.

In this regard, we investigate an exemplary sequence of fluvial terrace levels on the Adriatic side of the Marche Apennines. We combined field investigations, geomorphometric analyses, sedimentological analysis, and optically stimulated luminescence (OSL) dating to understand the interaction between the Pleistocene climate and the local differential uplift in controlling the fluvial aggradation-incision patterns. To achieve this, terrace treads were semi-automatically extracted from a high-resolution digital elevation model (DEM) using the surface classification model (SCM) procedure. This procedure was firstly developed and implemented for the study of marine terraces (Bowles and Cowgill, 2012) and was adapted here to detect potential fluvial terraces surfaces. Successively, for each terrace level, a cross-check in the field was carried out to determine: (i) the different terrace features (e.g., tread and alluvium), (ii) an estimation of deposit thickness, and (iii) the sampling of the latter for sedimentological analyses and OSL dating. Finally, the collective results are discussed in relation to climate and tectonics as key drivers for long term river valley evolution across the 10^4–10^5 yr timescale.

2. Study area

The Tesino River originates at about 700 m a.s.l within the hilly sector of the southern Marche piedmont zone of the Apennines flowing west to east into the Adriatic Sea at Grottammare (Fig. 1).

The Tesino catchment is characterized by a hilly landscape with a mean altitude of ~400 m a.s.l.. The maximum catchment height is at Mount Ascensione (1108 m a.s.l.) coinciding with the south-western drainage divide between the Tesino and Tronto catchments.

According to the climate data available for the nearby coastal zone that spans 1967–1996 (https://climatecharts.net, Zepner et al., 2021), the climate is humid subtropical (Cfa type following the Köppen classification) with a mean annual temperature of 13.9 °C. Seasonal means are 23.0 °C and 5.5 °C in July and January, respectively. The mean annual precipitation is 793.3 mm, with the wettest and driest months being November (93.6 mm) and July (38.5 mm), respectively.

2.1. Geological setting

The southern Marche is part of the peri-Adriatic foredeep basin and was formed between the Messinian and the Early Pliocene. It belongs to the Laga sedimentary basin filled by turbiditic sequences (Laga Fm) starting from the Messinian (e.g., Bartolini et al., 2003; Cosentino et al., 2010; Lanari et al., 2023). Since the Middle-Late Pliocene, the westernmost portion of the area experienced a regional uplift due to the propagation of the compressional front of the Apennines responsible for the emergence of the area. Meanwhile, in the easternmost portion, the presence of a subsiding basin gave rise to the deposition of a marine

sequence that rests unconformably on the underlying folded sediments (Laga Fm). Outcrops of Pliocene to Pleistocene marine sequences gently dip towards the ENE and occur extensively in the study area (Fig. 1).

In detail, the Plio-Pleistocene marine sequence exhibits a monocline with a gentle eastward dip primarily due to differential uplift (Amanti et al., 2020). This sequence consists of two distinct formations: the Argille Azzurre Fm (Pliocene - Lower Pleistocene) and the Fermo Fm (Lower Pleistocene). These formations exhibit varying lithological characteristics transitioning from pelites and sands at the base to intercalated layers of arenaceous and conglomeratic bodies, which are attributed to submarine fans and are notable for their calcarenitic clasts towards the top of the feature (Gentili et al., 2017). Conglomerates and gravels forming the top of the sequence are well exposed near the present coastline and are also known as "fanglomerates" according to Nesci and Savelli (2003). The western limit of the area is marked by the outcrop of the Messinian foredeep deposits. This variable strength favours the development of a smoother gently sloping hilly landscape morphology that alternates with areas of rough topographic relief including deeply incised streams and sub-vertical escarpments.

Finally, the presence of several main rivers draining towards the Adriatic Sea has led to the formation of thick alluvial deposits often terraced in four levels (e.g., Coltorti et al., 1991; Mayer et al., 2003; Wegmann and Pazzaglia, 2009; Nesci et al., 2012).

The Apennines coastal sector is characterized by a series of still active *E*-trending thrusts which are interrupted by strike-slip transverse ENE-WSW faults (Mirabella et al., 2008; Mazzoli et al., 2014; De Nardis et al., 2022; Console et al., 2023). Some authors suggested the activity of these faults as a possible cause for the fragmentation of the peri-Adriatic region into differently uplifted blocks (Bigi et al., 1995; Coltorti et al., 1996; Racano et al., 2020; Costa et al., 2021).

Regarding uplift rate determinations, several studies have obtained values using different methods ranging from 0.2 to 0.7 mm yr^{-1} and likely higher along the Apennines axis (Bigi et al., 1995; Cyr and Granger, 2008; Wegmann and Pazzaglia, 2009; Troiani and Della Seta, 2011; Sembroni et al., 2020; Delchiaro et al., 2021). Nevertheless, the role played of blind thrusts in driving anticlinal growth in the system remains unclear. Their possible influence on the anomalous altimetric distribution of the terrace levels within adjacent valleys is also unclear.

3. Methods

A geomorphological study of the area was carried out to map the fluvial terrace levels. A detailed geomorphological analysis based on remote sensing with field cross-checking was performed to identify and map different levels of fluvial terraces. The deposits of the different terrace levels were sampled for clast shape analysis (Supplementary material 3) and OSL dating. Finally, the terrace levels and dating results were incorporated with the modern river longitudinal profile for correlation. This then allowed the rates of Pleistocene valley incision to be quantified.

3.1. Remote sensing analysis

The remote sensing analysis was performed using freely available datasets including the geological and geomorphological maps at the scale of 10,000 made in 1999–2001 available for the Marche Region (https://www.regione.marche.it/Regione-Utile/Paesaggio-Territorio-Urbanistica/Cartografia/Repertorio/Cartageomorfologicaregionale10000).

The high-resolution LiDAR DTM (with a vertical accuracy of less than ±15 cm, a horizontal accuracy of ±30 cm, and a spatial resolution of 1 m) was acquired by the Italian Ministry for Environment, Land and Sea Protection for the 2008–2010 time interval. This is freely available for the main river valleys (Costabile, 2010; http://www.pcn.minambiente.it/mattm/progetto-piano-straordinario-di-telerilevamento/) and was used for the preliminary terrain analysis conducted with the MATLAB©-based TopoToolbox (Schwanghart and Scherler, 2014).

3.2. Semi-automatic extraction of terrace tread, along-valley correlations, and terrace level classification

A LiDAR DTM has also been adopted for the semi-automatic extraction using a MATLAB©-based TopoToolbox (Schwanghart and Scherler, 2014) of sub-planar and gently inclined topographic surfaces that hang along valley-sides and coincide with treads. The procedure partially follows the protocol used for the identification of ancient marine terraces described by Jara-Muñoz et al. (2016, 2019). The semi-automatic detection of low-relief and gently inclined smooth areas is based on a SCM developed by Bowles and Cowgill (2012), which uses a combination of topographic slope (SLP) and roughness (RG). The latter is defined as the standard deviation of the slope (Frankel and Dolan, 2007).

$$SCM = \left(\frac{SLP < SLPr}{SLPr} * 0.5\right) + \left(\frac{RG < RGr}{RGr} * 0.5\right) \quad (1)$$

Here, SLPr and RGr are defined as slope and roughness cut-offs, respectively.

The LiDAR DTM was first resampled at 5 m, and the distributions of slope and roughness were truncated respectively at 5° and the 0.9 quantile of RG (2.46). The resulting SCM values were filtered again below the 0.9 quantile (0.52). Since false positive classifications usually occur at valley bottoms and slopes, a 25-m buffer distance from the drainage network was considered to filter out such erroneous classifications. In this regard, a channel initiation threshold of 10^6 m^2 was used for extracting the drainage network. To extract the elevations above the thalweg, the resulting SCM patches were intersected with the values of a relative elevation model (REM), also known as a height above river (HAR) raster (Dilts et al., 2010). The planar features were classified according to their relative elevation values and cross-checked with the alluvial terrace deposits reported in the 1:10,000 geological and geomorphological maps of the Marche Region to check the capability of the semi-automatic method and detect the terrace remnants. This approach was considered applicable to the Tesino River because no knickpoints were detected along its longitudinal profile (Fig. 2). Furthermore, optical imagery was used for discriminating potential anthropic planar surfaces. Validation of the SCM performance in a fluvial tread semi-automatic extraction used confusion matrices (e.g., Stehman, 1997) in comparison with the literature and the final classification.

In detail, optical imagery includes the stereo-pairs of panchromatic aerial photos acquired by Volo GAI (1955) and Volo Italia (1988/1989) with a scale of 1:31.000 and 1:75.000, respectively (https://www.regione.marche.it/Regione-Utile/Paesaggio-Territorio-Urbanistica-Genio-Civile/Cartografia-e-informazioni-territoriali/Repertorio#Foto-Aeree). Furthermore, the WMS (Web Map Service) cloud services of the National Cartographic Portal (www.pcn.minambiente.it) offered colour orthophotos acquired in different periods. Specifically, we used (i) aerial orthophotos acquired over 1994–1998, 2000, and 2006 (scale 1:10,000), (ii) the aerial orthophotos acquired in 2008 and 2012 (spatial resolution of 50 cm/pixel), and (iii) the satellite imagery available on the Google Earth Pro platform at variable spatial resolution and acquired from 2001 to 2022.

Finally, the points corresponding to the obtained terrace treads were projected along the Tesino River longitudinal profile.

3.3. Geomorphological field survey and sediment sampling

Field surveys were conducted to: (i) cross-check and confirm the fluvial terrace treads identified from the preliminary remote and terrain analysis; (ii) identify and characterize terrace deposits, and, eventually, estimate the deposit thickness; (iii) sample the terrace deposits for

Table 1
Numeric ages from Quaternary fluvial deposits of the Marche Apennines. Basin abbreviations: C Cesano, Ch Chienti, E Esino, M Musone, P Potenza, T Tenna, F Foglia, Fr Frasassi Gorge (for locations see Fig. 1a).

Terrace name	Numeric ages from Quaternary fluvial deposits of the Marche Apennines				
	Basin	Source	Age	MIS	Methodology
–	Fr	Cyr and Granger (2008)*	750,000 ± 260,000	19	$^{26}Al/^{10}Be$
2nd level	Fr	Taddeucci et al. (1992)**	160,000 ± 10,000	6	$^{230}Th/^{234}U$
?	E	Materazzi et al. (2022)	>44460***	–	^{14}C
?	T	Cilla et al. (1996)	>44000***	–	^{14}C
3rd level	Mt	Calderoni et al. (1994)	>44,000	2/3	^{14}C
3rd level	Mt	Calderoni et al. (1994)	>43,000	2/3	^{14}C
3rd level	C	Nesci et al. (1995)	42,000 ± 4000	2/3	^{14}C
3rd level	E	Calderoni et al. (1991)	41,400 ± 4000	2/3	^{14}C
3rd level	C	Calderoni et al. (1991)	37,300 ± 2200	2/3	^{14}C
3rd level	C	Calderoni et al. (1991)	35,600 ± 1800	2/3	^{14}C
3rd level	E	Calderoni et al. (1991)	32,700 ± 1200	2/3	^{14}C
3rd level	E	Calderoni et al. (1991)	32,500 ± 1200	2/3	^{14}C
3rd level	C	Calderoni et al. (1991)	32,500 ± 1200	2/3	^{14}C
3rd level	E	Calderoni et al. (1991)	31,800 ± 1100	2/3	^{14}C
3rd level	C	Calderoni et al. (1991)	31,700 ± 1050	2/3	^{14}C
3rd level	M	Wegmann and Pazzaglia (2009)	30,980 ± 240	2/3	^{14}C
3rd level	E	Calderoni et al. (1991)	30,200 ± 900	2/3	^{14}C
3rd level	Ch	Damiani and Moretti (1968)	30,150 ± 1200	2/3	^{14}C
3rd level	M	Wegmann and Pazzaglia (2009)	26,810 ± 290	2	^{14}C
3rd level	Ch	Damiani and Moretti (1968)	26,800 ± 700	2	^{14}C
3rd level	M	Wegmann and Pazzaglia (2009)	26,540 ± 90	2	^{14}C
3rd level	M	Wegmann and Pazzaglia (2009)	25,260 ± 210	2	^{14}C
3rd level	E	Calderoni et al. (1991)	23,500 ± 400	2	^{14}C
3rd level	F	Mencucci et al. (2003)	23,500 ± 120	2	^{14}C
3rd level	M	Wegmann and Pazzaglia (2009)	23,020 ± 170	2	^{14}C
3rd level	E	Materazzi et al. (2022)	21,900 ± 300	2	^{14}C
3rd level	T	Cilla et al. (1996)	20,020 ± 150	2	^{14}C
3rd level	M	Wegmann and Pazzaglia (2009)	16,730 ± 90	2	^{14}C
3rd level	E	Alessio et al. (1979)	15,250 ± 160	2	^{14}C
3rd level	E	Alessio et al. (1979)	14,700 ± 150	2	^{14}C

*Chronological measurement of cosmogenic nuclide ^{26}Al:^{10}Be burial age for sediments in Grotta della Madonna - Frasassi Gorge (Ancona, Italy). **Chronological measurement carried out on speleothems from Grotta del Fiume - Grotta Grande del Vento karst system at Frasassi Gorge (Ancona, Italy). ***On the limit result for AMS radiocarbon dating methodology.

successive laboratory sedimentological analyses and OSL dating.

Here, OSL sampling requires great care to prevent the sample from being exposed to light because the luminescence signal could be reduced or even reset, thus a meticulous sampling strategy was adopted. First, when selecting a site, it is important to sample levels with original sedimentary structures, thus avoiding bioturbations and post-depositional alterations. Once a suitable site has been identified, it is important to clean the exposure carefully. Moreover, samples are typically taken from at least one meter below the surface to minimize the effects of cosmic radiation thus avoiding the risk of rejuvenated ages. Finally, homogeneous sand-dominated layers or pockets of minimum 30 cm thickness were targeted for sampling; samples were collected using a metal tube inserted horizontally into a vertical face using a hammer. From the same level where it was sampled, an additional 500–800 g of sediment was collected to determine the natural radioactivity as well as to evaluate the moisture content. Gravel samples were also collected over the tread of the selected dating sites for a rapid shape analysis of the three terrace levels as detailed in the Supplementary materials 3.

3.4. Optically stimulated luminescence dating

Three samples (S4, S7, S9) from three different levels of fluvial terrace were collected for luminescence burial dating. The luminescence dating was performed by the Laboratory of the Institute of Geological Sciences, University of Bern, Switzerland. Feldspar minerals with a grain size of 63–150 μm were extracted for equivalent dose (ED) measurements using standard separation protocol (e.g., Gaar et al., 2014; Trauerstein et al., 2014). Luminescence measurements were performed using two Risø TL/OSL DA-20 readers with a calibrated $^{90}Sr/^{90}Y$ beta source (dose rates of 0.093 Gy/s – sample S4, and 0.079 Gy/s – samples S7-S9) including one equipped with a single-grain attachment (Bøtter-Jensen, 1997).

Natural feldspar EDs were measured using post-IR IRSL 150 °C protocol (Reimann and Tsukamoto, 2012; Table 1 in supplementary material 1). The reliability of the protocol was checked by conducting Dose Recovery Test measurements on artificially bleached samples (two days' exposure under a Sunlux Ambience UV lamp). For all samples, the recovered dose after removal of the residual signal was within 10 % of the given dose (within the uncertainty) for both the IR_{50} and the post-IR_{150} signal. Replicate ED measurements were conducted on 24 aliquots with a 1 mm diameter (samples S7 and S4) or using pseudo–single grain analyses (i.e., 10–15 grains per hole, with two disks with 100 holes each, sample S9) based on sedimentological observations, thus suggesting a potentially more complex depositional history (see Section 4.2 and Fig. 6 for detailed description).

Fading measurements were performed following the approach of Auclair et al. (2003) on five aliquots/sample (two full SG disks for S9). U^{238}, Th^{232}, and K^{40} concentrations (Table 2 in the supplementary material 1) of bulk sediment were measured using high-resolution gamma spectrometry (Department of Chemistry and Biochemistry at University of Bern, Switzerland; Preusser and Kasper, 2001); Ra^{226} was also measured to check for potential disequilibrium in the U^{238} decay chain. Following no observation of disequilibrium, U^{238}, Th^{232}, and K^{40} concentrations were input in the dose rate and age calculator (DRAC; Durcan et al., 2015) for dose rate determination (Table 2 in the supplementary material 1).

The IR_{50} signal was used for final age determination because of its better bleaching properties (Colarossi et al., 2015). The moderate overdispersion (below 25 %; Table 2 in supplementary material 1) and the relatively symmetrical distribution of replicated ED measurements (Fig. 1 in supplementary material 1) suggest no significant effect of complex depositional history for the IR_{50} signal. Final equivalent doses

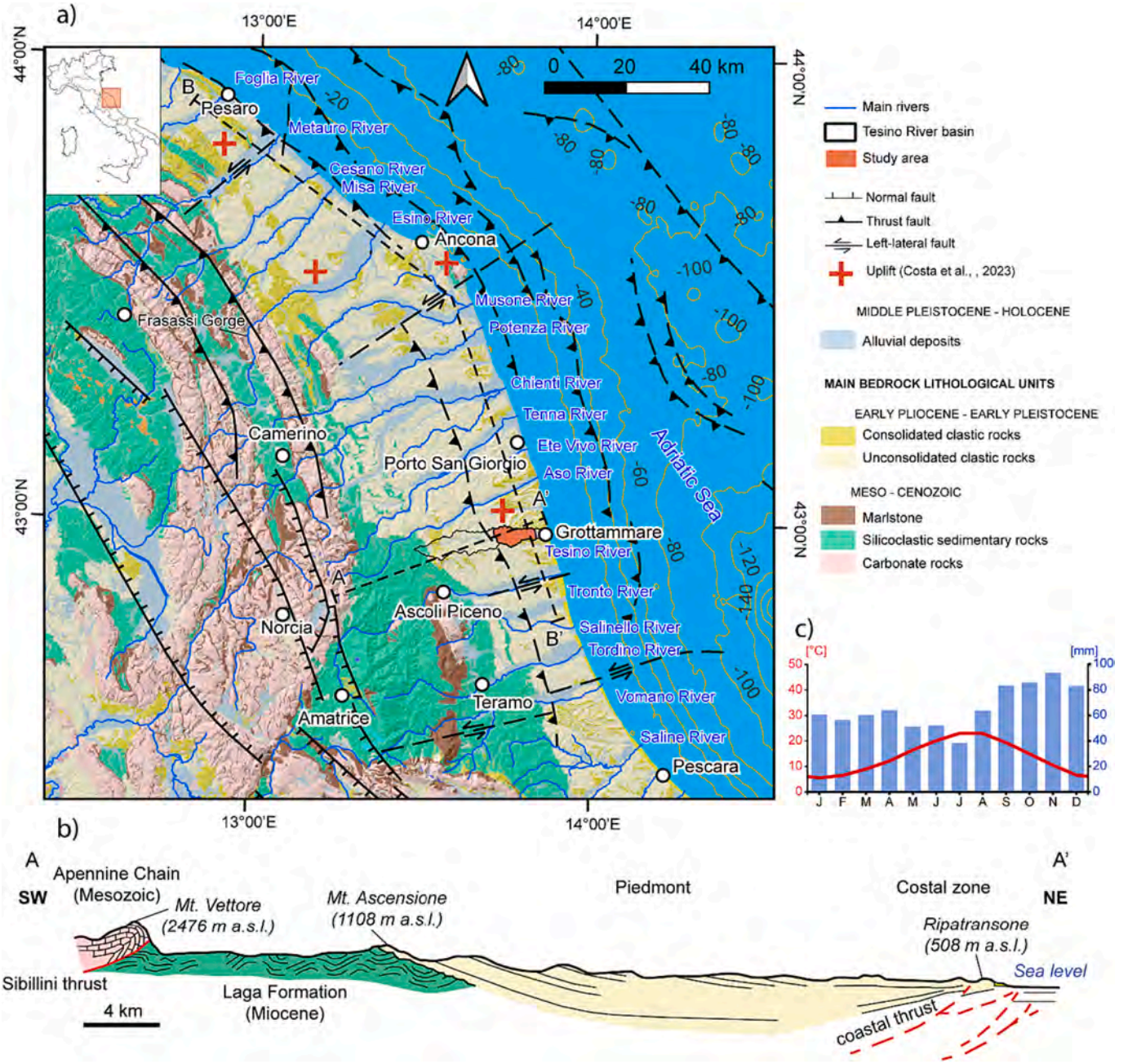

Fig. 1. a) Lithological map of the central Apennines of Italy (Bucci et al., 2022). The reported faults are taken from the Individual Seismogenic Sources from the DISS catalogue (version 3.3.0; 2021), Costa et al. (2023), and Della Seta et al. (2008). The location of the Tesino River basin within the southern portion of the Marche Piedmont Zone of the Apennines (sensu Della Seta et al., 2008) is reported. The hillshade is derived from the 1 arc sec Shuttle Radar Topographic Mission DEM (SRTM, CGIAR-CSI, 2006) with a WGS84 projection. b) The geological section modified after Buccolini et al. (2010) is shown. c) The climate chart relative to the Falconara locality close to the city of Ancona for the period 1967–1996 is also reported (Zepner et al., 2021).

were computed using the Central Age Model (CAM; Galbraith et al., 1999). The apparent age was then obtained by dividing the CAM ED by the sample individual natural dose rate. Final fading-corrected ages were then calculated by applying the approach by Huntley and Lamothe (2011) for samples with a natural signal within the linear part of dose response curve (DRC) (S4) or following Kars et al. (2008) for samples with natural signal plotting within the non-linear part of the DRC (S7 and S9). For the latter approach, a mean natural signal was calculated, and a single common laboratory DRC was reconstructed from all the Ln/Tn and Lx/Tx values measured at the pseudo-SG scale. Calculations were performed using the R-Luminescence package (Kreutzer et al., 2022) and the following functions: calc_FadingCorr, analyse_Fading Measurement (Kreutzer and Burow, 2022), and calc_Huntley2006 (King and Burow, 2022).

4. Results

4.1. Plano-altimetric distribution of the fluvial terrace staircases

The preliminary recognition of the terrace treads using the semi-automatic extraction is the first step in the identification of the terrace levels as well as for delimiting the present alluvial plain.

The general accuracy of the SCM in predicting outcrops of terrace treads is generally good and increases for younger terrace levels with a

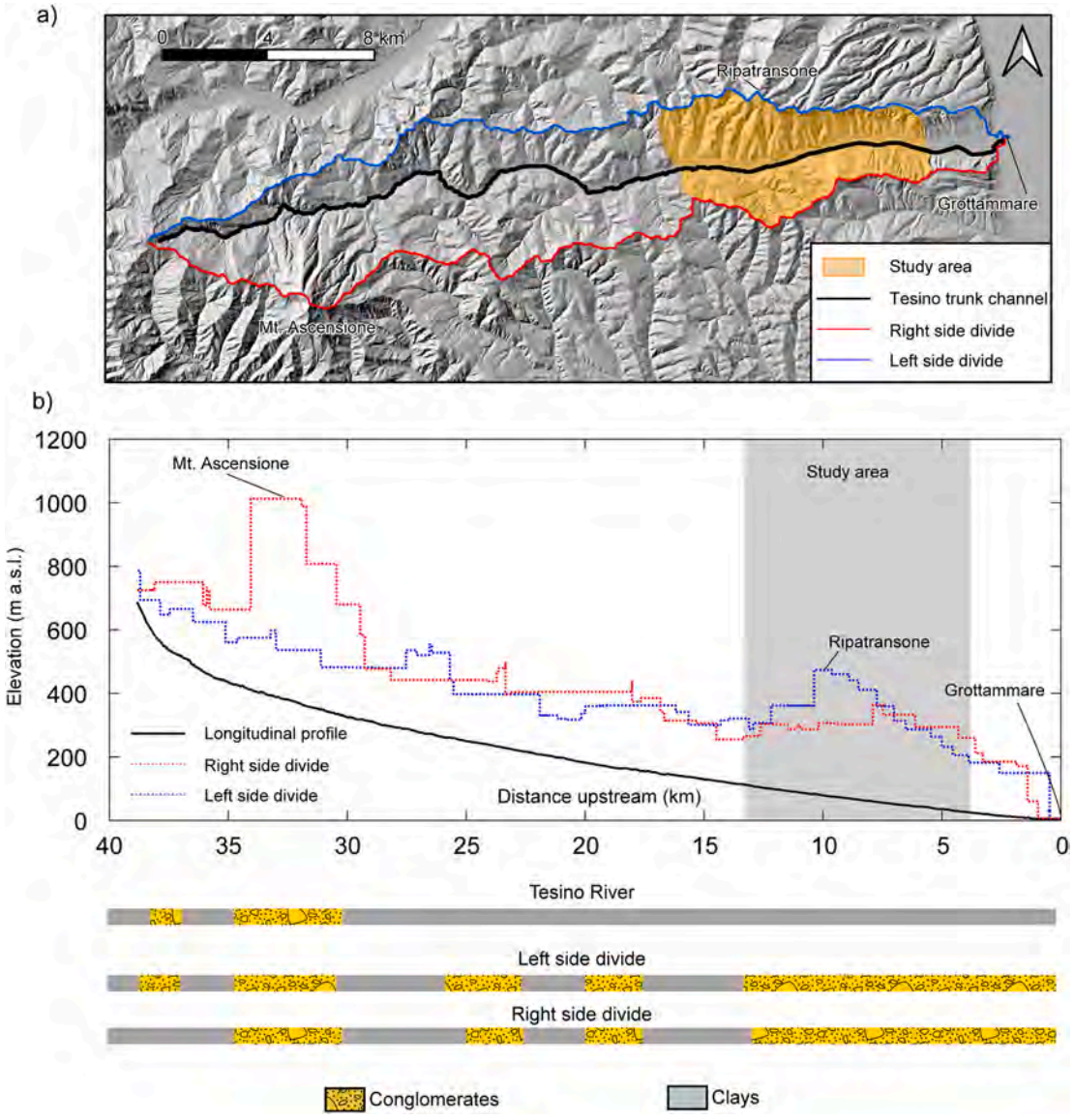

Fig. 2. (a) The entire Tesino basin and the location of the study area, distinguishing right and left side drainage divides; (b) the longitudinal profile of the Tesino River and the topographic profiles of the divides.
The hillshade view was derived from the DTM (Costabile, 2010).

maximum with the alluvial plain (for details see Figs. 11, 12, and 13 in the supplementary material 2). Moreover, literature shows that polygons overestimate the presence of fluvial treads because they fail to distinguish between the tread and the alluvium outcrop. Indeed, the false positive classifications are greater in the literature than with SCM—especially for older terrace levels.

The field survey was crucial to classify the fluvial deposits as fill terraces (sensu Pazzaglia, 2013) distinguishing between the top depositional surface (i.e., tread) and the underlying terraced deposit (i.e., terraced alluvium) (Fig. 3a). Indeed, only about 3.7 % of the study area is occupied by these deposits, and these can be distinguished into three different levels as we can appreciate in the projection of the terrace treads along the longitudinal profile (Fig. 3b). The lowest level was recognized as an active and rather wide alluvial plain (Holocene in age as reported by the Geological and Geomorphological maps of the Marche region).

The 1st level (T1) and the 2nd level (T2) preserve the top depositional surfaces in each mapped remnant despite their extension being somewhat restricted. Conversely, the 3rd level (T3) preserves small tread remnants versus the extent of the outcropping alluvium. Especially along the left valley side, several tributaries were recognized as active gullies and V-shaped valleys illustrating significant erosion of the pelitic lithotype. Indeed, the latter characterizes about 83 % of the outcropping lithofacies in the study area followed by sandy lithofacies (7 %), pelitic/sandy (4 %), and conglomeratic (3 %). Furthermore, the length of left-bank tributaries (looking downstream) is significantly greater in comparison to the right-bank ones (Fig. 3b). The terraced deposits have been recognized essentially along the left valley (Fig. 3a), while the present-day alluvial plain is easily recognizable on both sides.

The Tesino River longitudinal profile shows a regular concave-up geometry without knickpoints (Fig. 2). The right and left drainage divides are at about 300 m a.s.l. and decrease regularly towards the mouth at Grottammare. The greatest anomaly can be observed along the left-side divide in Ripatransone, where it reaches ca. 500 m a.s.l. (Fig. 2). The projection of the terrace treads along the river longitudinal profile (Fig. 3b) shows that the T1, T2, and T3 terrace levels can be detected about 140–110 m, 90–60 m, and 45–15 m above thalweg, respectively. The terrace treads show a regular along-valley trend parallel to the river

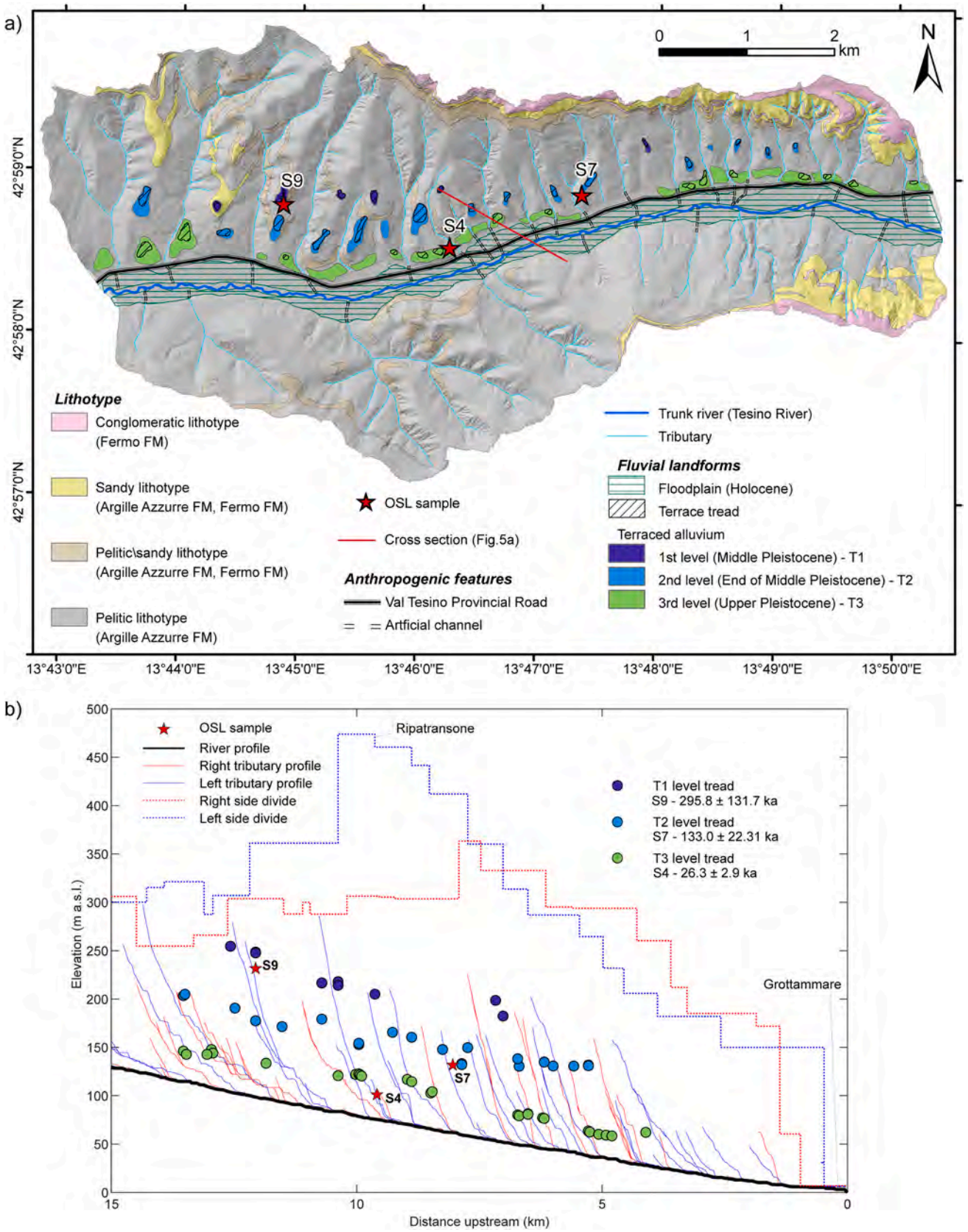

Fig. 3. a) Map of the Middle-Late Pleistocene fluvial terraces in the study area superimposed to the four main lithotypes. The hillshade view was derived from Costabile, 2010; http://www.pcn.minambiente.it/mattm/progetto-piano-straordinario-di-telerilevamento/). The coordinate reference system is WGS84. b) Longitudinal profile of the Tesino River including left and right tributaries along which each terrace tread with the dated samples is projected. The left and right drainage divide profiles are also reported.

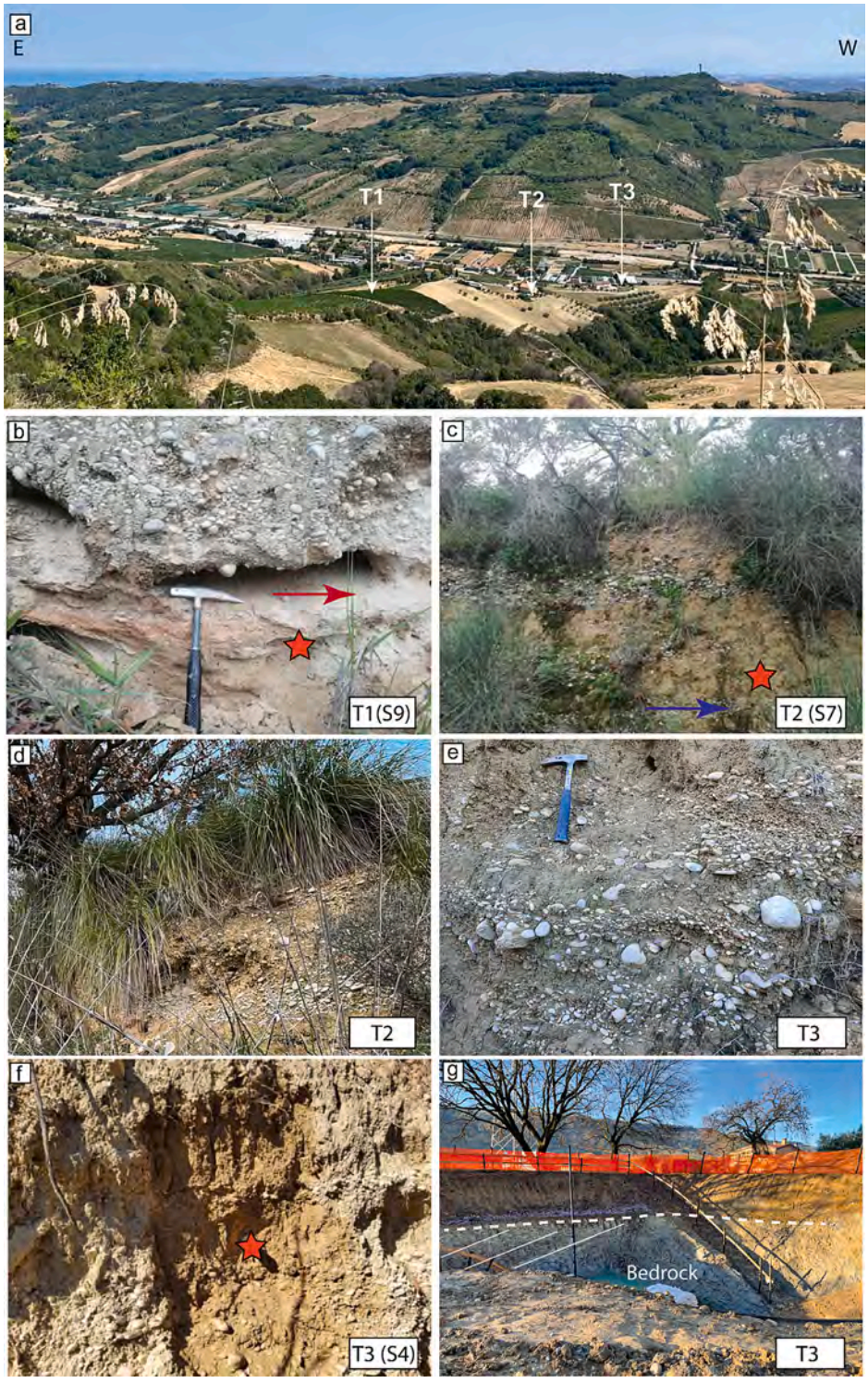

Fig. 4. a) A panoramic view of the middle sector of the Tesino river valley; b) sampled T1 deposit (S9); c) sampled T2 deposit (S7); d) the coarsening upward deposit observed in T2; e) the T3 deposit; f) sample location of T3 (S4); and g) the unconformity between the Argille Azzurre FM and the terrace deposits belonging to the 3rd level (T3). The red arrow (in b and d) illustrates out flow direction in an outcrop perpendicular to the valley axis. The blue arrow (in c) indicates flow direction in an outcrop parallel with the valley axis. Red stars (in b, c, and f) indicate the OSL sampling points.

profile, thus confirming the height above thalweg as a good detector of the different terrace levels.

The field survey facilitated characterization of sedimentological features that indicate two main types of deposits for each terrace level (Fig. 4). The first deposit is characterized by cross-stratified gravel, moderately sorted and well rounded, with occasional sand-dominated layers. A coarsening upward succession can be locally observed. Moreover, the clasts exhibit imbricated sedimentary structures observable along outcrops parallel to the valley axis. The second type of deposit is clast-supported and lithologically heterogeneous with sub-rounded and poorly sorted pebbles; well bedded-laminated and sandy-mud levels can occasionally be observed. In addition, the clasts show imbrication in

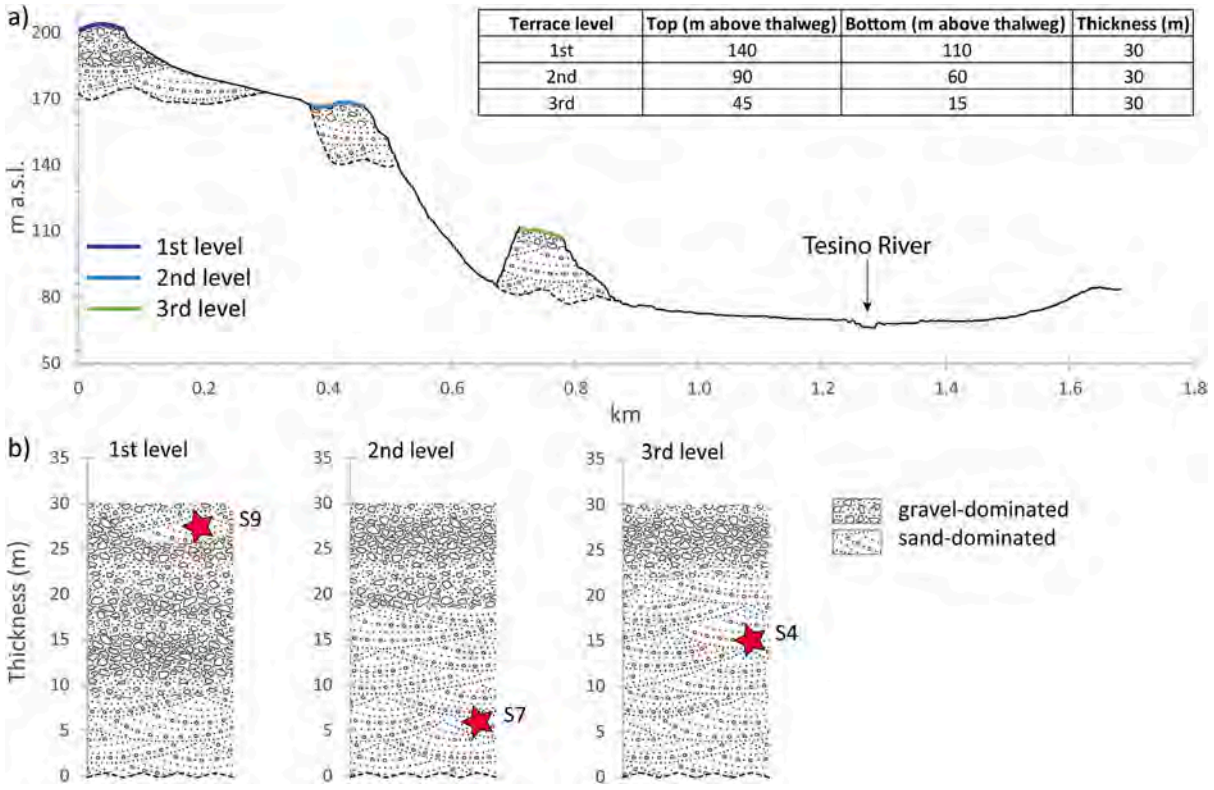

Terrace level	Top (m above thalweg)	Bottom (m above thalweg)	Thickness (m)
1st	140	110	30
2nd	90	60	30
3rd	45	15	30

Fig. 5. a) The cross section mapped in Fig. 3a representing the tread and the alluvium of each level; b) schematic stratigraphic logs representing the three levels (following Nesci et al., 2012) and the position of the OSL samples.

outcrops perpendicular to the valley axis.

The T1 outcrops (Fig. 4b) preserve essentially the clast-supported deposit where poorly sorted cobbles tens of centimetres in size have been locally observed above a 30-cm laminated muddy layer; T2 (Fig. 4c and d) presents both the facies, although the clast-supported one is partially preserved and recognizable through the increasing size of sub-rounded pebbles. Finally, the T3 deposit is characterized only by cross-stratified deposits (Fig. 4f) with an increasing pebble size over the terrace tread (Fig. 4e).

Considering the field checks of the basal erosional surfaces of the terraced alluvium, the estimated alluvium thickness of each terrace is about 30 m; see previously published descriptions and the cross-section reported in Fig. 5. In detail, the specific thickness of each deposit has been determined only considering the field survey observations along the main left tributary valleys, where the terraced deposits frequently crop out.

4.2. Chronology of the fluvial terrace staircase

Three OSL samples (S9, S7, and S4) were collected for each terrace level (Fig. 5). S9 was sampled about 137 m above thalweg, where the 1st level terrace was recognized. S7 was collected at about 64 m above thalweg, sampling the sandiest part of the 2nd level terrace. Finally, S4 was sampled at about 32 m above the thalweg where we again recognized the sandiest portion belonging to the 3rd level terrace (Fig. 5).

Table 2 summarizes the ages of each terrace level obtained by the OSL dating method. The oldest sample S9 belongs to the 1st level, and it was dated to 295.8 ± 131.7 ka. S7 was collected from the 2nd level and dated to 133.1 ± 22.31 ka. S4 belongs to the 3rd level with an age of 26.3 ± 2.9 ka. The oldest sample is affected by the greatest error (~45 % relative error), which we tentatively attribute to the large variability in the pseudo-SG luminescence signals responses (Ln/Tn and Lx/Tx) that were directly used to apply the Kars et al. (2008) fading-correction model. The mean natural signal is closer to the saturation field after fading correction, and potential uncertainties in the natural response of this feldspar sample in the high dose range (ex. >1 kGy). We thus recommend considering this age as preliminary pending further confirmation from independent methods.

5. Discussion

This study focuses on the lower sector of the Tesino basin as an

Table 2
OSL analysis report.

Sample ID	Lat./Long.	Elevation (m a.s.l.)	Depth (m)	Terrace level	U (ppm)	Th (ppm)	^{40}K (%)	Dose rate (Gy/ka)	Apparent age (ka)	Fading corrected age (ka)[a]
S9	45.980°/ 13.748°	231	1.5	T1	1.51 ± 0.13	4.02 ± 0.20	1.25 ± 0.06	2.47 ± 0.20	165.7 ± 13.6	295.8 ± 131.7
S7	42.981°/ 13.789°	131	1.5	T2	1.77 ± 0.11	5.22 ± 0.26	1.04 ± 0.05	2.45 ± 0.20	88.3 ± 7.3	133.1 ± 22.31
S4	42.976°/ 13.771°	102	1.5	T3	1.75 ± 0.10	6.36 ± 0.32	1.20 ± 0.06	2.68 ± 0.21	19.1 ± 1.8	26.3 ± 2.9

[a] Fading correction performed following Huntley and Lamothe (2001) for S4 and following Kars et al. (2008) for S7 and S9.

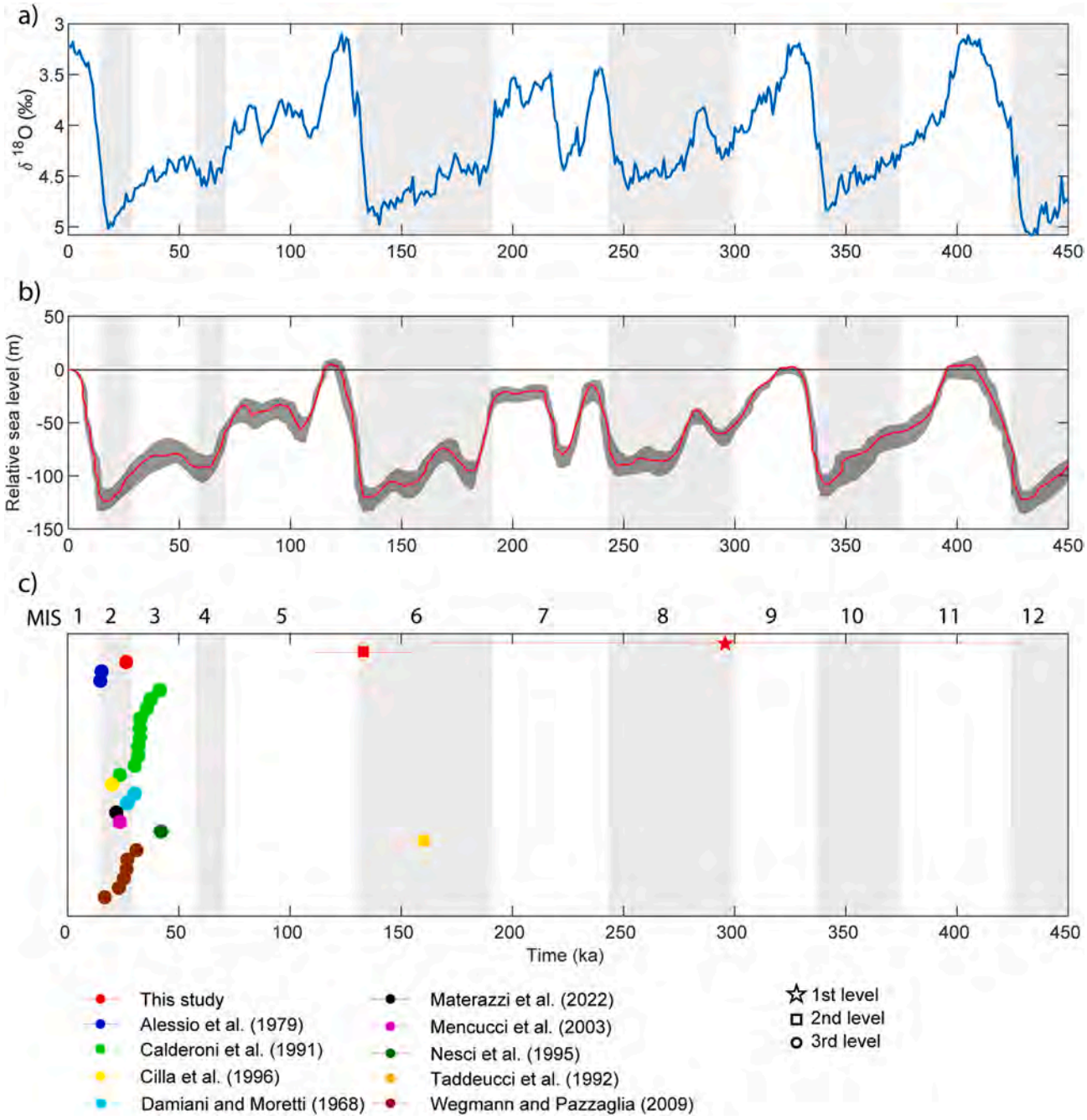

Fig. 6. a) Oxygen isotope curve of globally distributed benthic records from Lisiecki and Raymo (2005). b) The global eustatic curve updated for the last 500 ka (Bintanja et al., 2005). c) The age distribution of available data for the Marche piedmont zone of the Apennines including the present study ages.

exemplary landscape where a well-preserved staircase of fluvial terraces can provide better comprehension of the interaction among the late Quaternary climatic and tectonic evolution of the Marche Apennines. Here, the low-rate tectonic activity documented in the area and the lithological configuration characterized by a highly erodible bedrock, in association with the climate changes, give the possibility to study their mutual contribution to the sedimentary flux.

5.1. *Climate insights from the fluvial terrace staircase*

The OSL chronology of the fluvial terrace levels related to the study area (Fig. 6) highlights how fluvial sedimentation has generally occurred during the late Quaternary main cold phases as already suggested by several studies (Damiani and Moretti, 1968; Alessio et al., 1979; Coltorti, 1981; Coltorti et al., 1991; Nesci et al., 1995). In detail, the 3rd level terrace (26.3 ± 2.9 ka) was mainly deposited during MIS 2 in agreement with other results available in the literature (Damiani and Moretti, 1968; Alessio et al., 1979; Calderoni et al., 1991; Nesci et al., 1995; Calderoni et al., 1996; Cilla et al., 1996; Coltorti and Farabollini, 2008; Wegmann and Pazzaglia, 2009; Materazzi et al., 2022) when the associated relative sea level was −102 ± 6 m (Fig. 6) corresponding to a mouth approximately 37 km away from the present location (Fig. 1).

The 2nd level (133.1 ± 22.31 ka) was formed during MIS 6, and the associated relative sea level was −119 ± 12 m (Fig. 6) corresponding to a mouth approximately 40 km away from the present (Fig. 1). Such a date is the first that comes directly from fluvial deposits and agrees with the previously proposed indirect chronology based on numerical dating of speleothems from the Frasassi karst system (Taddeucci et al., 1992).

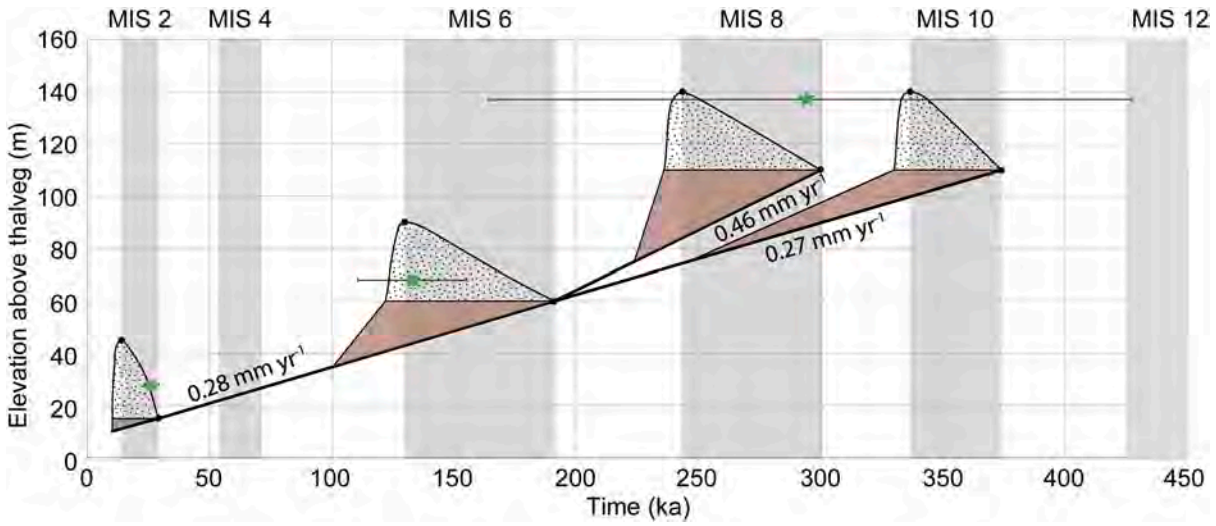

Fig. 7. Tesino River bed height through time, thus highlighting the deposition-incision cycles related to the terrace levels superimposed upon the overall trend of incision. The age-elevation coordinates related to the present study OSL samples are reported.

In the 1st level, the large uncertainty of the sample S9 (295.8 ± 131.7 ka) does not allow a clear correlation with a specific MIS, but only supports a Middle Pleistocene age of the terrace—sometimes between late MIS 6 to MIS 12. However, we tentatively associate the sedimentation phase with MIS 8 or 10 in agreement with what was assumed on morpho-stratigraphic basis by Wegmann and Pazzaglia (2009) and Nesci et al. (2010, 2012), assuming a cold-driven aggradation. In addition, an age older than MIS 6 can be hypothesized because that age is already associated with the T2 terrace level. Nevertheless, since we are close to the limit of OSL dating range, the age can be potentially consolidated in future work with other techniques with longer dating ranges (for example, cosmogenic burial dating or Electron Spin Resonance). The associated relative sea level was at least −60 ± 7 m (Fig. 6) corresponding to a mouth approximately 20 km away from the present (Fig. 1).

The cold-climate driven aggradation is strictly related to the position of the coastline during the sea low stands. Indeed, it was located 20 to 40 km away from the present one because of the wide extension of the Adriatic continental shelf (Mayer et al., 2003; Storms et al., 2008). According to Schanz et al. (2018), the aggradation phase is most commonly associated with increased sediment supply. Indeed, in the middle regions of the catchment areas as in our study area, conditions promoting meteoric weathering occurred along slopes during cooling phases. This led to high sediment production that reached the valley floors either by gravity or through runoff. In this context, the presence of highly erodible bedrock could have favoured the weathering, thus increasing the consequent sediment production (Schanz and Montgomery, 2016). Conversely, during warming phases, vegetation gradually re-colonizes the slopes, thus resulting in a significant reduction in the flux of sediments reaching the valley floors. In turn, there is a decrease in the dispersed energy of the watercourses, thus amplifying their erosive potential. Moreover, each terrace level is characterized by two types of deposits indicating changes of flow regime. Such an observation is well known in the northern Marche area, and it was interpreted as a possible transition from braided stream facies (*Fb*; sensu Nesci et al., 2012) to alluvial fan facies (*af*; sensu Nesci et al., 2012). This change was attributed to temperature lowering in the final stage of cold phases by Nesci et al. (2010). The dynamic sedimentological relationships of alluvial fan/river interactions in response to climate change has also been confirmed by the broader work of Mather et al. (2017). In our study area, while such changes were identified in the field, there is insufficient sedimentological data to confirm what is hypothesized in the northern Marche. However, it is possible to preliminarily correlate the alluvial fan facies *af* to the clast-supported deposits described in the results as well as the *Fb* to the cross-stratified deposits characterized by well-rounded gravel. Specifically, regarding *Fb* facies (sensu Nesci et al., 2012), we have assessed the thickest deposits for T3 to be about 20–25 m. This was about 18 m for T2, and not directly observed for T1 (Fig. 6b). The *af* facies (sensu Nesci et al., 2012) of T1 and T2 were observed in the sampled outcrops as well as along the cross sections of the main left tributaries. Conversely, the *af* facies of T3 is poorly and locally preserved, and its occurrence is inferred only where the treads still occur. A general thickness decrease of *af* can be observed among the terrace level. In this regard, the *af* deposition can be linked to the tributary sedimentary contribution.

5.2. Uplift rate determination from terraces staircase

The Marche Apennines are characterized by a series of active E-trending thrusts disrupted by strike-slip transverse ENE-WSW faults (Mirabella et al., 2008; Mazzoli et al., 2014; De Nardis et al., 2022; Console et al., 2023). Such setting gives rise to a regional uplift rate ranging from 0.2 to 0.7 mm yr^{-1} and likely higher along the Apennines axis (Bigi et al., 1995; D'Agostino et al., 2001; Cyr and Granger, 2008; Wegmann and Pazzaglia, 2009; Troiani and Della Seta, 2011; Sembroni et al., 2020; Delchiaro et al., 2021). This uplift pattern is further influenced by local variations resulting from the fragmentation of the peri-Adriatic region into distinct blocks experiencing differing uplift rates (as elaborated in Bigi et al., 1995; Coltorti et al., 1996; Costa et al., 2021).

To calculate the long-term bedrock incision rate, interpreted as a regional uplift rate, we applied the model of Pederson et al. (2006) to the dated terrace levels assuming that the sedimentation likely occurred during cold climate phases. The corresponding MIS for each terrace levels are MIS 8/10, 6 and 2 for T1, T2, and T3, respectively. In this regard, the actual thalweg of the Tesino river as well as the other terrace level strath surface are carved into the bedrock (Fig. 5a). This is evidence of active uplift making it possible to consider such terraces as strath erosional terraces characterized by a thick layer of sediment (up to 30 m). However, Zondervan et al. (2022) reported that extracting incision rates from terraces can be problematic due to the Sadler Effect—an apparent dependence of incision rates on measured time intervals that apparently increases towards the present—as well as to the position of dates within the cycle of aggradation.

To remove those biases, rate calculations should be integrated over Quaternary terraces representing at least one glacial-interglacial cycle of

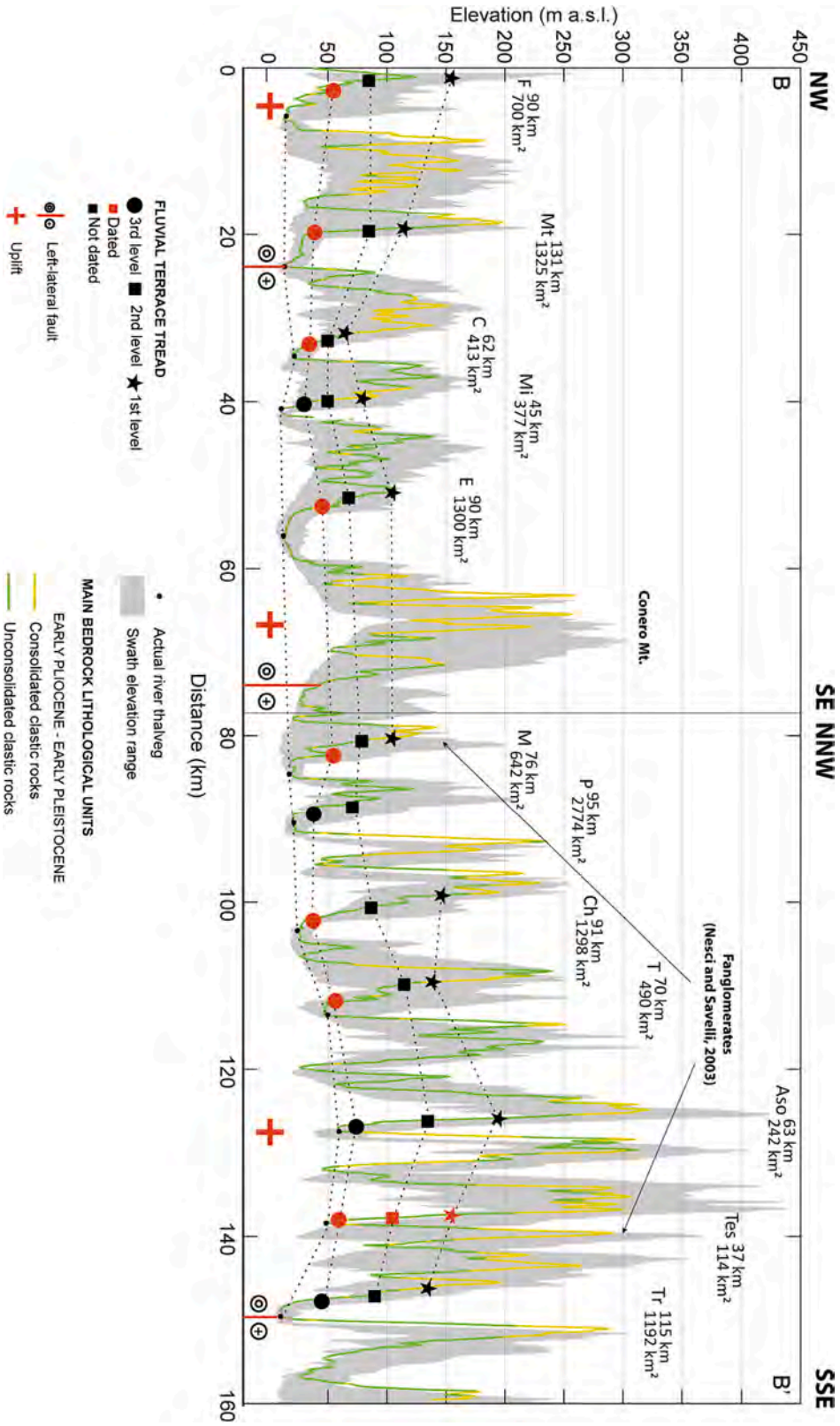

Fig. 8. Topographic profiles orthogonal to the direction of the trunk-valleys showing the height distribution of terraces throughout the Marche Apennines. The profile trace is reported in Fig. 1. The swath width is 5000 m.

incision and aggradation (Wegmann and Pazzaglia, 2002). This approach must further consider the full range of terrace aggradation (Schanz and Montgomery, 2016). In this regard, we focused on three glacial-interglacial cycles from MIS 2 to MIS 8/10. In addition, our dates in association with available literature dates for the 3rd level allowed us to precisely locate the start and the end of the aggradation phase to MIS 2. The scarcity of dates suggests that future studies on the topic of older levels are necessary to better constrain the aggradation history.

Table 3
Single basins with terrace level heights corresponding to the B-B′ and C-C′ cross sections of Figs. 1 and 8.

Basin	River Elevation (m a.s.l.)	Terrace level	Terrace Elevation above thalweg (m)	Reference
Tronto (Tr)	10	1st	120	Della Seta et al. (2008)
		2nd	75	
		3rd	30	
Tesino (Tes)	48	1st	140	This study
		2nd	90	
		3rd	45	
Aso (Aso)	59	1st	180	Marche region Geomorphological map[a]
		2nd	120	
		3rd	60	
Tenna (T)	50	1st	124	Marche region Geomorphological map[a]
		2nd	100	
		3rd	40	
Chienti (Ch)	24	1st	120	Coltorti et al. (1991)
		2nd	72	
		3rd	22	
Potenza (P)	21	1st	?	Calderoni et al. (1996)
		2nd	56	
		3rd	20	
Musone (M)	17	1st	90	Wegmann and Pazzaglia (2009)
		2nd	64	
		3rd	40	
Esino (E)	12	1st	90	Nesci et al. (2012)
		2nd	53	
		3rd	30	
Misa (Mi)	10	1st	65	Nesci et al. (2012)
		2nd	35	Iacobucci et al. (2022)
		3rd	15	
Cesano (C)	22	1st	50	Nesci et al. (2012)
		2nd	35	
		3rd	20	
Metauro (Mt)	13	1st	100	Nesci et al. (2012)
		2nd	70	
		3rd	24	
Foglia (F)	15	1st	140	Nesci et al. (2010)
		2nd	70	
		3rd	40	

[a] From the Geological and Geomorphological maps at the scale of 10,000 of the Marche Region. Available at the link: https://www.regione.marche.it/Regione-Utile/Paesaggio-Territorio-Urbanistica/Cartografia/Repertorio/Cartageomorfologicaregionale10000. Scientific Coordinator: F. Florindo (2005–2006).

Nevertheless, it can be assumed that the sedimentation begins with the beginning of the cold phases and ends with the end of the corresponding cold period.

Fig. 7 shows the height of the valley floor over time and the cycles of aggradation and incision associated with each terrace level. In this regard, the T1 age error is very large, and both MIS 8 and MIS 10 were considered in computing the incision rate.

The resulting incision rates are between about 0.5 and 0.3 mm yr^{-1} considering the period between MIS 8 or MIS 10 for the T1 sedimentation phase, and the beginning of MIS 6 for the T2 sedimentation phase, respectively. The period between MIS 6 and MIS 2 shows a rate of about 0.3 mm yr^{-1}. Since the lower incision rate of 0.3 mm yr^{-1} for the earlier inter-terrace interval (T1-T2) is consistent with the rate resulting for the later interval (T2-T3), it is good evidence that the older of the two possibilities (MIS 10 rather than MIS 8) is more likely to be correct for T1 level. These rates are generally consistent with the estimations along the Adriatic flank of the Apennines (Bigi et al., 1995; Cyr and Granger, 2008; Wegmann and Pazzaglia, 2009; Troiani and Della Seta, 2011; Sembroni et al., 2020).

Regarding the effect of the local uplift, Fig. 8 shows the main terrace staircases of the Marche Apennines projected along swath topographic transepts drawn parallel to the present coastline. The details of the terrace levels are reported in Table 3. Along the profiles, we see an unequal height distribution of the same terrace levels with a positive anomaly between the Tenna and Tesino valleys and near the Foglia river valley. This is consistent with the anomaly recorded on the elevation of the current thalwegs and the elevation distribution along the swath profile showing maximum values in the same areas. The bedrock erodibility does not appear to play a role in the development of these anomalies because fluvial staircases develop mostly on erodible lithologies. The location of the differentially-uplifted areas agrees with the position of left-lateral faults (Costa et al., 2023) that disrupted the Marche Apennines into blocks.

6. Conclusions

This work confirms the value of fluvial terraces in the Marche piedmont zone as geomorphic indicators for climatic and tectonic studies. The terraces are an important source of data in this case study and reveal both climate and uplift-driven fluvial system responses in the area. The availability of high-resolution LiDAR, supported by field analysis, contributed to precise identification and classification of the fluvial terraces. Moreover, the application of the procedure for the semi-automatic extraction of terrace treads and its good prediction performance allowed us to identify possible markers that were cross-checked with previous studies and field surveys. The results and OSL dating within the Tesino valley allow us to present the following:

1 - An enhanced map of the Pleistocene fluvial terrace surfaces distinguished and classified into three levels;
2 - Independent confirmation and integration of the previously documented terrace chronology from OSL ages at least for two main terrace levels. This consolidates the existing chronology available in the study area especially in the higher age range (10^4 to 10^5 yr);
3 - Calculation of new uplift rates, consistent with the data already present in the area;
4 - Correlation of fluvial aggradation with main Pleistocene cold stages.

Supplementary data to this article can be found online at https://doi.org/10.1016/j.geomorph.2023.108971.

CRediT authorship contribution statement

Michele Delchiaro: Conceptualization, Methodology, Software, Formal analysis, Investigation, Writing – original draft, Visualization. **Giulia Iacobucci:** Conceptualization, Methodology, Formal analysis, Investigation, Writing – original draft, Visualization. **Marta Della Seta:** Conceptualization, Methodology, Writing – review & editing, Supervision. **Natacha Gribenski:** Methodology, Formal analysis, Writing – review & editing. **Daniela Piacentini:** Conceptualization, Methodology, Writing – review & editing, Supervision, Funding acquisition. **Valeria Ruscitto:** Formal analysis, Investigation, Writing – original draft, Visualization. **Marta Zocchi:** Formal analysis, Investigation, Writing – original draft, Visualization. **Francesco Troiani:** Conceptualization, Methodology, Writing – review & editing, Supervision, Project administration, Funding acquisition.

Declaration of competing interest

The authors declare that they have no conflict of interest.

Data availability

Geological and Geomorphological maps at the scale of 10,000 made in 1999-2001 for the Marche Region are available at the link https://www.regione.marche.it/Regione-Utile/Paesaggio-Territorio-Urbanistica/Cartografia/Repertorio/Cartageomorfologicaregionale10000. The high-resolution LiDAR DTM is available at the link http://www.pcn.minambiente.it/mattm/progetto-piano-straordinario-di-telerilevamento/. The code

for the semi-automatic extraction and preliminary level classification of terrace treads is available as supplementary material. The functions used in the analysis are available in TopoToolbox (https://github.com/wschwanghart/topotoolbox). Details on the OSL sampling site and general info on the deposits are provided in the text of this article. The samples themselves have been obviously disrupted by the analytical procedure.

Acknowledgments

This study was carried out within the RETURN Extended Partnership and received funding from the European Union Next-GenerationEU (National Recovery and Resilience Plan – NRRP, Mission 4, Component 2, Investment 1.3 – D.D. 1243 2/8/2022, PE0000005). This research has been supported by Sapienza University of Rome through the Project "Progetti di Ateneo 2020" no. Grant. RM120172A260A846 (P.I.: F. Troiani) and the Project "Progetti di Ateneo 2022" no. Grant. RM1221816764C043 (P.I. D. Piacentini). The Authors thank the Italian Ministry of Environment (National Geoportal at http://www.pcn.minambiente.it/) for providing the high-resolution Digital Elevation Model derived from LiDAR dataset. The Authors also thank the Regione Marche, Direzione Ambiente e Risorse Idriche (https://www.regione.marche.it/Regione-Utile/Paesaggio-Territorio-Urbanistica/Cartografia/Repertorio/Cartatecnicanumerica110000) for providing the topographic dataset (CTR Regione Marche, scala 1:10,000). The Authors gratefully acknowledge three anonymous reviewers for their deep and stimulating revision of the manuscript, as well as to the editorial work by the Editor Martin Stokes.

References

Alessio, M., Allegri, L., Coltorti, M., Cortesi, C., Deiana, G., Dramis, F., Improta, S., Petrone, V., 1979. Depositi tardowürmiani nell'alto Bacino dell'Esino (Appennino Marchigiano)-Datazione con il ^{14}C. Geogr. Fis. Din. Quat. 2, 203–205.

Amanti, M., Muraro, C., Roma, M., Chiessi, V., Puzzilli, L.M., Catalano, S., Tallini, M., 2020. Geological and geotechnical models definition for 3rd level seismic microzonation studies in Central Italy. Bull. Earthq. Eng. 18, 5441–5473. https://doi.org/10.1007/s10518-020-00843-x.

Auclair, M., Lamothe, M., Huot, S., 2003. Measurement of Anomalous Fading for Feldspar IRSL Using SAR: Radiation Measurement, 37, pp. 487–492. https://doi.org/10.1016/S1350-4487(03)00018-0.

Bartolini, C., D'Agostino, N., Dramis, F., 2003. Topography, exhumation, and drainage network evolution of the Apennines. Episodes J. Int. Geosci. 26 (3), 212–216. https://doi.org/10.18814/epiiugs/2003/v26i3/010.

Bigi, S., Cantalamessa, G., Centamore, E., Didaskalou, P., Dramis, F., Farabollini, P., Potetti, M., 1995. La fascia periadriatica marchigiano-abruzzese dal Pliocene medio ai tempi attuali: evoluzione tettonico-sedimentaria e geomorfologica. Studi Geol. Camerti 1, 37–49.

Bintanja, R., Van De Wal, Oerlemans, J., 2005. Modelled atmospheric temperatures and global sea levels over the past million years. Nature 437 (7055), 125–128. https://doi.org/10.1038/nature03975.

Blum, M.D., Valastro Jr., S., 1994. Late Quaternary sedimentation, lower Colorado River, Gulf Coastal Plain of Texas. Geol. Soc. Am. Bull. 106 (8), 1002–1016. https://doi.org/10.1130/0016-7606(1994)106<1002:LQSLCR>2.3.CO;2.

Bøtter-Jensen, L., 1997. Luminescence techniques: instrumentation and methods. Radiat. Meas. 27 (5–6), 749–768. https://doi.org/10.1016/S1350-4487(97)00206-0.

Bowles, C.J., Cowgill, E., 2012. Discovering marine terraces using airborne LiDAR along the Mendocino-Sonoma coast, northern California. Geosphere 8 (2), 386–402. https://doi.org/10.1130/GES00702.1.

Bridgland, D.R., 2000. River terrace systems in north-west Europe: an archive of environmental change, uplift and early human occupation. Quat. Sci. Rev. 19 (13), 1293–1303. https://doi.org/10.1016/S0277-3791(99)00095-5.

Bridgland, D.R., Howard, A.J., White, M.J., White, T.S., Westaway, R., 2015. New insight into the Quaternary evolution of the River Trent, UK. Proc. Geol. Assoc. 126 (4–5), 466–479. https://doi.org/10.1016/j.pgeola.2015.06.004.

Bridgland, D.R., Westaway, R., 2008. Preservation patterns of Late Cenozoic fluvial deposits and their implications: results from IGCP 449. Quat. Int. 189 (1), 5–38. https://doi.org/10.1016/j.quaint.2007.08.036.

Brocard, G.Y., Van Der Beek, Bourlès, D.L., Siame, L.L., Mugnier, J.L., 2003. Long-term fluvial incision rates and postglacial river relaxation time in the French Western Alps from 10Be dating of alluvial terraces with assessment of inheritance, soil development and wind ablation effects. Earth Planet. Sci. Lett. 209 (1–2), 197–214. https://doi.org/10.1016/S0012-821X(03)00031-1.

Bucci, F., Santangelo, M., Fongo, L., Alvioli, M., Cardinali, M., Melelli, L., Marchesini, I., 2022. A new digital lithological map of Italy at the 1: 100 000 scale for geomechanical modelling. Earth Syst. Sci. Data 14 (9), 4129–4151. https://doi.org/10.5194/essd-14-4129-2022.

Buccolini, M., Gentili, B., Materazzi, M., Piacentini, T., 2010. Late Quaternary geomorphological evolution and erosion rates in the clayey peri-Adriatic belt (central Italy). Geomorphology 116 (1–2), 145–161. https://doi.org/10.1016/j.geomorph.2009.10.015.

Bucher, W.H., 1932. "Strath" as a Geomorphic Term. Science 75 (1935), 130–131.

Bull, W.B., 1991. Geomorphic Responses to Climatic Change.

Bull, W.B., 2007. Tectonic Geomorphology of Mountains. Blackwell Publishing, Malden, MA. https://doi.org/10.1002/9780470692318, 316 pp.

Burbank, D.W., Leland, J., Fielding, E., Anderson, R.S., Brozovic, N., Reid, M.R., Duncan, C., 1996. Bedrock incision, rock uplift and threshold hillslopes in the northwestern Himalayas. Nature 379 (6565), 505–510. https://doi.org/10.1038/379505a0.

Calderoni, G., Coltorti, M., Dramis, F., Magnatti, M., Cilla, G., 1991. Sedimentazione fluviale e variazioni climatiche nell'alto bacino del Fiume Esino durante il Pleistocene superiore. Fenomeni di erosione e alluvionamento degli alvei fluviali. Università di Ancona, Ancona, pp. 171–190.

Calderoni, G., Nesci, O., Pergolini, C., Savelli, D., 1994. Last-glacial terrace alluvium in the Metauro River basin: some remarks about new radiometric ages. Il Quaternario 7, 607–611.

Calderoni, G., Cilla, G., Dramis, F., Farabollini, P., 1996. Dinamica fluviale olocenica nella media valle del Fiume Potenza (Italia Centrale). Geogr. Fis. Din. Quat. 19, 19–28.

Campbell, M.R., 1929. The river system: a study in the use of technical geographic terms. J. Geogr. 28 (3), 123–128. https://doi.org/10.1080/00221342908984773.

Cerrone, C., Vacchi, M., Fontana, A., Rovere, A., 2021. Last Interglacial sea-level proxies in the Western Mediterranean. Earth Syst. Sci. Data 13 (9), 4485–4527. https://doi.org/10.5194/essd-13-4485-2021.

CGIAR-CSI, 2006. Applying GeoSpatial Science for Sustainable Future. CGIAR-Consortium for Spatial Information. www2.jpl.nasa.gov/srtm/.

Cilla, G., Coltorti, M., Dramis, F., Farabollini, P., Gentili, B., Pambianchi, G., 1996. Fluvial sedimentation during the early Holocene in the Marchean valleys (Central Italy). Il Quaternario 9 (2), 459–464.

Colarossi, D., Duller, G.A.T., Roberts, H.M., Tooth, S., Lyons, R., 2015. Comparison of paired quartz OSL and feldspar post-IR IRSL dose distributions in poorly bleached fluvial sediments from South Africa. Quat. Geochronol. 30, 233–238. https://doi.org/10.1016/j.quageo.2015.02.015.

Coltorti, M., 1981. Lo stato attuale delle conoscenze sul Pleistocene e il Paleolitico inferiore e medio della regione marchigiana. Atti 1 Convegno Beni Culturali e Ambientali delle Marche, Numana, 8–10 maggio 1981, pp. 63–122.

Coltorti, M., Nanni, T., 1987. La bassa valle del finne Esino; geomorfologia, idrogeologia e neotettonica. Boll. Soc. Geol. Ital. 106 (1), 35–51.

Coltorti, M., Consoli, M., Dramis, F., Gentili, B., Pambianchi, G., 1991. Evoluzione geomorfologica delle piane alluvionali delle Marche centro-meridionali. Geogr. Fis. Din. Quat. 14 (1), 87–100.

Coltorti, M., Dramis, F., 1988. The significance of stratified slope waste deposits in the quaternary Umbria marche apennines (Central italy). in Zeit. fur Geomorphologie, n. F., suppl. Bol. 71, 59–70.

Coltorti, M., Farabollini, P., Gentili, B., Pambianchi, G., 1996. Geomorphological evidence for anti-Apennine faults in the Umbro-Marchean Apennines and in the peri-Adriatic basin, Italy. Geomorphology 15 (1), 33–45. https://doi.org/10.1016/0169-555X(95)00117-N.

Console, R., Vannoli, P., Falcone, G., 2023. Magnitude distribution and clustering properties of the 3D Seismicity in Central Apennines (Italy). Geophys. J. Int. https://doi.org/10.1093/gji/ggad017.

Cosentino, D., Cipollari, P., Marsili, P., Scrocca, D., 2010. Geology of the central Apennines: a regional review. J. Virtual Explor. 36 (11), 1–37. https://doi.org/10.3809/jvirtex.2009.00223.

Costa, M., Chicco, J., Invernizzi, C., Teloni, S., Pierantoni, P.P., 2021. Plio–Quaternary structural evolution of the outer sector of the Marche Apennines South of the Conero Promontory, Italy. Geosciences 11 (5), 184. https://doi.org/10.3390/geosciences11050184.

Costa, M., Invernizzi, C., Penza, G., Teloni, S., Pierantoni, P.P., 2023. The seismotectonic role of transversal structures in the Plio-Quaternary evolution of the External Marche Apennines (Italy). J. Geol. Soc., jgs2023-002 https://doi.org/10.1144/jgs2023-002.

Costabile, S., 2010. Geoportale Nazionale: il Piano Straordinario di Telerilevamento per l'Ambiente. GEOmedia 14 (3). http://www.pcn.minambiente.it/.

Cyr, A.J., Granger, D.E., 2008. Dynamic equilibrium among erosion, river incision, and coastal uplift in the northern and central Apennines, Italy. Geology 36 (2), 103–106. https://doi.org/10.1130/G24003A.1.

D'Agostino, N., Jackson, J.A., Dramis, F., Funiciello, R., 2001. Interactions between mantle upwelling, drainage evolution and active normal faulting: an example from the central Apennines (Italy). Geophys. J. Int. 147 (2), 475–497. https://doi.org/10.1046/j.1365-246X.2001.00539.x.

Damiani, A.V., Moretti, A., 1968. Segnalazione di un episodio lacustre würmiano nell'alta valle del Chienti (Marche).

De Nardis, R., Pandolfi, C., Cattaneo, M., Monachesi, G., Cirillo, D., Ferrarini, F., Lavecchia, G., 2022. Lithospheric double shear zone unveiled by microseismicity in a region of slow deformation. Sci. Rep. 12 (1), 21066. https://doi.org/10.1038/s41598-022-24903-1.

Delchiaro, M., Della Seta, M., Martino, S., Dehbozorgi, M., Nozaem, R., 2019. Reconstruction of river valley evolution before and after the emplacement of the giant Seymareh rock avalanche (Zagros Mts., Iran). Earth Surf. Dyn. 7 (4), 929–947. https://doi.org/10.5194/esurf-7-929-2019.

Delchiaro, M., Fioramonti, V., Della Seta, M., Cavinato, G.P., Mattei, M., 2021. Fluvial inverse modeling for inferring the timing of Quaternary uplift in the Simbruini range

(Central Apennines, Italy). Trans. GIS 25 (5), 2455–2480. https://doi.org/10.1111/tgis.12833.
Delchiaro, M., Iacobucci, G., Troiani, F., Della Seta, M., Ballato, P., Aldega, L., 2022. Morphoevolution of the Seymareh landslide-dam lake system (Zagros Mountains, Iran): Implications for Holocene climate and environmental changes. Geomorphology 413, 108367. https://doi.org/10.1016/j.geomorph.2022.108367.
Delchiaro, M., Della Seta, M., Martino, S., Nozaem, R., Moumeni, M., 2023. Tectonic deformation and landscape evolution inducing mass rock creep driven landslides: the Loumar case-study (Zagros Fold and Thrust Belt, Iran). Tectonophysics 846, 229655. https://doi.org/10.1016/j.tecto.2022.229655.
Della Seta, M., Del Monte, M., Fredi, P., Lupia Palmieri, E., 2004. Quantitative morphotectonic analysis as a tool for detecting deformation patterns in soft-rock terrains: a case study from the southern Marches, Italy/Analyse morphotectonique quantitative dans une province lithologique enregistrant mal les déformations: les Marches méridionales, Italie. Geomorphol. Relief, Process. Environ. 10 (4), 267–284.
Della Seta, M., Fredi, P., Lupia Palmieri, E., Nesci, O., Savelli, D., Troiani, F., 2005. River terraces in the Fiume Tronto drainage basin, Marche Region: a contribution to morphotectonic investigations. Geogr. Fis. Din. Quat. 123–135.
Della Seta, M., Del Monte, M., Fredi, P., Miccadei, E., Nesci, O., Pambianchi, G., Troiani, F., 2008. Morphotectonic evolution of the Adriatic piedmont of the Apennines: an advancement in the knowledge of the Marche-Abruzzo border area. Geomorphology 102 (1), 119–129. https://doi.org/10.1016/j.geomorph.2007.06.018.
Di Bucci, D., Mazzoli, S., Nesci, O., Savelli, D., Tramontana, M., De Donatis, M., Borraccini, F., 2003. Active deformation in the frontal part of the Northern Apennines: insights from the lower Metauro River basin area (northern Marche, Italy) and adjacent Adriatic off-shore. J. Geodyn. 36 (1–2), 213–238. https://doi.org/10.1016/S0264-3707(03)00048-6.
Dilts, T.E., Yang, J., Weisber, P.J., 2010. Mapping Riparian Vegetation with LiDAR Data: Predicting Plant Community Distribution Using Height Above River and Flood Height. ArcUser. Winter 2010. http://www.esri.com/news/arcuser/0110/files/mapping-with-lidar.pdf.
Dramis, F., Bisci, C., 1986. Aspetti geomorfologici del territorio marchigiano. In: Da "La Geologia delle Marche" (Volume speciale di Studi Geologici Camerti), pp. 99–103.
Durcan, J.A., King, G.E., Duller, G.A.T., 2015. DRAC: Dose Rate and Age Calculator for trapped charge dating. Quat. Geochronol. 28, 54–61. https://doi.org/10.1016/j.quageo.2015.03.012.
Dutta, S., Suresh, N., Kumar, R., 2012. Climatically controlled Late Quaternary terrace staircase development in the fold-and-thrust belt of the Sub Himalaya. Palaeogeogr. Palaeoclimatol. Palaeoecol. 356, 16–26. https://doi.org/10.1016/j.palaeo.2011.05.006.
Fanucci, F., Moretti, E., Nesci, O., Savelli, D., Veneri, F. (Eds.), 1996. Tipologia dei terrazzi vallivi ed evoluzione del rilievo nel versante adriatico dell'Appennino centro-settentrionale. Il Quaternario, 9, pp. 255–258.
Frankel, K.L., Dolan, J.F., 2007. Characterizing arid region alluvial fan surface roughness with airborne laser swath mapping digital topographic data. J. Geophys. Res. Earth 112 (F2). https://doi.org/10.1029/2006JF000644.
Gaar, D., Lowick, S., Preusser, F., 2014. Performance of different luminescence approaches for the dating of known-age glaciofluvial deposits from northern Switzerland. Geochronometria 41 (1), 65–80. https://doi.org/10.2478/s13386-013-0139-0.
Galbraith, R.F., Roberts, R.G., Laslett, G.M., Yoshida, H., Olley, J.M., 1999. Optical dating of single and multiple grains of quartz from Jinmium rock shelter, northern Australia: part I, experimental design and statistical models. Archaeometry 41, 339–364. https://doi.org/10.1111/j.1475-4754.1999.tb00987.x.
Gao, H., Li, Z., Ji, Y., Pan, B., Liu, X., 2016. Climatic and tectonic controls on strath terraces along the upper Weihe River in central China. Quatern. Res. 86 (3), 326–334. https://doi.org/10.1016/j.quascirev.2015.12.003.
Gentili, B., Pambianchi, G., Aringoli, D., Materazzi, M., Giacopetti, M., 2017. Pliocene-Pleistocene geomorphological evolution of the Adriatic side of central Italy. Geol. Carpath. 68 (1), 6. https://doi.org/10.1515/geoca-2017-0001.
Hu, Z., Pan, B., Wang, J., Cao, B., Gao, H., 2012. Fluvial terrace formation in the eastern Fenwei Basin, China, during the past 1.2 Ma as a combined archive of tectonics and climate change. J. Asian Earth Sci. 60, 235–245. https://doi.org/10.1016/j.jseaes.2012.09.016.
Huang, W.L., Yang, X.P., Li, A., Thompson, J.A., Zhang, L., 2014. Climatically controlled formation of river terraces in a tectonically active region along the southern piedmont of the Tian Shan, NW China. Geomorphology 220, 15–29. https://doi.org/10.1016/j.geomorph.2014.05.024.
Huntley, D.J., Lamothe, M., 2001. Ubiquity of anomalous fading in K-feldspars and the measurement and correction for it in optical dating. Can. J. Earth Sci. 38, 1093–1106. https://doi.org/10.1139/cjes-38-7-1093.
Iacobucci, G., Piacentini, D., Troiani, F., 2022. Enhancing the identification and mapping of fluvial terraces combining geomorphological field survey with land-surface quantitative analysis. Geosciences 12 (11), 425. https://doi.org/10.3390/geosciences12110425.
Jara-Muñoz, J., Melnick, D., Strecker, M.R., 2016. TerraceM: a MATLAB® tool to analyze marine and lacustrine terraces using high-resolution topography. Geosphere 12 (1), 176–195. https://doi.org/10.1130/GES01208.1.
Jara-Muñoz, J., Melnick, D., Pedoja, K., Strecker, M.R., 2019. TerraceM-2: a Matlab® interface for mapping and modeling marine and lacustrine terraces. Front. Earth Sci. 255 https://doi.org/10.3389/feart.2019.00255.
Kars, R.H., Wallinga, J., Cohen, K.M., 2008. A new approach towards anomalous fading correction for feldspar IRSL dating—tests on samples in field saturation. Radiat. Meas. 43 (2–6), 786–790. https://doi.org/10.1016/j.radmeas.2008.01.021.
King, G.E., Burow, C., 2022. calc_Huntley2006: Apply the Huntley (2006) model. Function version 0.4.1. In: Kreutzer, S., Burow, C., Dietze, M., Fuchs, M.C., Schmidt, C., Fischer, M., Friedrich, J., Mercier, N., Philippe, A., Riedesel, S., Autzen, M., Mittelstrass, D., Gray, H.J., Galharret, J. (Eds.), Luminescence: Comprehensive Luminescence Dating Data Analysis. R package Version 0.9.19. https://CRAN.R-project.org/package=Luminescence.
Kreutzer, S., Burow, C., 2022. analyse_FadingMeasurement: analyse fading measurements and returns the fading rate per decade (g-value). Function version 0.1.21. In: Kreutzer, S., Burow, C., Dietze, M., Fuchs, M.C., Schmidt, C., Fischer, M., Friedrich, J., Mercier, N., Philippe, A., Riedesel, S., Autzen, M., Mittelstrass, D., Gray, H.J., Galharret, J. (Eds.), Luminescence: Comprehensive Luminescence Dating Data Analysis. R Package Version 0.9.19. https://CRAN.R-project.org/package=Luminescence.
Kreutzer, S., Burow, C., Dietze, M., Fuchs, M.C., Schmidt, C., Fischer, M., Friedrich, J., Mercier, N., Philippe, A., Riedesel, S., Autzen, M., Mittelstrass, D., Gray, H.J., Galharret, J., 2022. Luminescence: Comprehensive Luminescence Dating Data Analysis. R Package Version 0.9.19. https://CRAN.R-project.org/package=Luminescence.
Lanari, R., Reitano, R., Faccenna, C., Agostinetti, N.P., Ballato, P., 2023. Surface and crustal response to deep subduction dynamics: Insights from the Apennines, Italy. Tectonics 42, e2022TC007461. https://doi.org/10.1029/2022TC007461.
Leopold, L.B., Wolman, M.G., Miller, J.P., Wohl, E.E., 1964. Fluvial processes in geomorphology. W.H. Freeman, San Francisco.
Lewin, J., Gibbard, P.L., 2010. Quaternary river terraces in England: forms, sediments and processes. Geomorphology 120 (3–4), 293–311. https://doi.org/10.1016/j.geomorph.2010.04.002.
Lipparini, T., 1939. I terrazzi fluviali delle Marche. Comitato nazionale per la geografia.
Lisiecki, L.E., Raymo, M.E., 2005. A Pliocene-Pleistocene stack of 57 globally distributed benthic δ18O records. Paleoceanography 20 (1). https://doi.org/10.1029/2004PA001071.
Maddy, D., 1997. Uplift-driven valley incision and river terrace formation in southern England. J. Quat. Sci. 12 (6), 539–545. https://doi.org/10.1002/(SICI)1099-1417(199711/12)12:6<539::AID-JQS350>3.0.CO;2-T.
Maddy, D., Bridgland, D., Westaway, R., 2001. Uplift-driven valley incision and climate-controlled river terrace development in the Thames Valley, UK. Quat. Int. 79 (1), 23–36. https://doi.org/10.1016/S1040-6182(00)00120-8.
Madritsch, H., Preusser, F., Fabbri, O., 2012. Climatic and tectonic controls on the development of the River Ognon terrace system (eastern France). Geomorphology 151, 126–138. https://doi.org/10.1016/j.geomorph.2012.01.023.
Materazzi, M., Bufalini, M., Dramis, F., Pambianchi, G., Gentili, B., Di Leo, M., 2022. Active tectonics and paleoseismicity of a transverse lineament in the Fabriano valley, Umbria-Marche Apennine (central Italy). Int. J. Earth Sci. 111 (5), 1539–1549. https://doi.org/10.1007/s00531-022-02198-x.
Mather, A.E., Stokes, M., Whitfield, E., 2017. River terraces and alluvial fans: the case for an integrated Quaternary fluvial archive. Quat. Sci. Rev. 166, 74–90. https://doi.org/10.1016/j.quascirev.2016.09.022.
Mayer, L., Menichetti, M., Nesci, O., Savelli, D., 2003. Morphotectonic approach to the drainage analysis in the North Marche region, central Italy. Quat. Int. 101, 157–167. https://doi.org/10.1016/S1040-6182(02)00098-8.
Mazzoli, S., Macchiavelli, C., Ascione, A., 2014. The 2013 Marche offshore earthquakes: new insights into the active tectonic setting of the outer northern Apennines. J. Geol. Soc. London 171 (4), 457–460. https://doi.org/10.1144/jgs2013-091.
Mencucci, D., Colantoni, P., Nesci, O., 2003. The Foglia river alluvial system (northern marche) and its relation to the late quaternary evolution of the central adriatic shelf. Alpine Mediterr. Quat. 16 (1), 35–42.
Merritts, D.J., Vincent, K.R., Wohl, E.E., 1994. Long river profiles, tectonism, and eustasy: a guide to interpreting fluvial terraces. J. Geophys. Res. Solid Earth 99 (B7), 14031–14050. https://doi.org/10.1029/94JB00857.
Mirabella, F., Barchi, M., Lupattelli, A., Stucchi, E., Ciaccio, M.G., 2008. Insights on the seismogenic layer thickness from the upper crust structure of the Umbria-Marche Apennines (central Italy). Tectonics 27 (1). https://doi.org/10.1029/2007TC002134.
Necea, D., Fielitz, W., Kadereit, A., Andriessen, P.A.M., Dinu, C., 2013. Middle Pleistocene to Holocene fluvial terrace development and uplift-driven valley incision in the SE Carpathians, Romania. Tectonophysics 602, 332–354. https://doi.org/10.1016/j.tecto.2013.02.039.
Nesci, O., Savelli, D., 1990. Valley terraces in the Northern Marche Apennines (Central Italy): cyclic deposition and erosion. Giornale di Geol. Ser. 3° 52 (1/2), 189–195.
Nesci, O., Savelli, D., 1991. Successioni alluvionali terrazzate nell'Appennino nord-marchigiano. Geogr. Fis. Din. Quat. 14 (1), 149–162.
Nesci, O., Savelli, D., 2003. Diverging drainage in the Marche Apennines (central Italy). Quat. Int. 101, 203–209. https://doi.org/10.1016/S1040-6182(02)00102-7.
Nesci, O., Savelli, D., Mengarelli, D., 1990. I terrazzi vallivi del 1 ordine nei bacini dei Fiumi Metauro e Foglia (Appennino Marchigiano). Geogr. Fis. Din. Quat. 13 (1), 63–73.
Nesci, O., Savelli, D., Calderoni, G., Elmi, C., Veneri, F., 1995. Le antiche piane di fondovalle nell'Appennino nord-marchigiano. Mem. Soc. Geol. Ital. 53, 293–312.
Nesci, O., Savelli, D., Troiani, F., 2010. Late-Quaternary alluvial fans in the northern Marche Apennines: implications of climate changes. Alp. Mediterr. Quat. 23 (1), 145–156.
Nesci, O., Savelli, D., Troiani, F., 2012. Types and development of stream terraces in the Marche Apennines (central Italy): a review and remarks on recent appraisals. Géomorphologie 18 (2), 215–238. https://doi.org/10.4000/geomorphologie.9838.
Pazzaglia, F.J., 2013. Fluvial terraces. In: Shroder, J., Wohl, E. (Eds.), Treatise on Geomorphology. Academic Press, San Diego, CA, vol. 9, Fluvial Geomorphology, pp. 379–412. https://doi.org/10.1016/B978-0-12-374739-6.00248-7.

Pederson, J.L., Anders, M.D., Rittenhour, T.M., Sharp, W.D., Gosse, J.C., Karlstrom, K.E., 2006. Using fill terraces to understand incision rates and evolution of the Colorado River in eastern Grand Canyon, Arizona. J. Geophys. Res. Earth 111 (F2). https://doi.org/10.1029/2004JF000201.

Penck, A., Brückner, E., 1909. Die alpen im Eiszeitalter, vol. 3. Tauchnitz.

Preusser, F., Kasper, H.U., 2001. Comparison of dose rate determination using high-resolution gamma spectrometry and inductively coupled plasma-mass spectrometry. Ancient TL 19 (1), 19–23.

Racano, S., Fubelli, G., Centamore, E., Bonasera, M., Dramis, F., 2020. Geomorphological detection of surface effects induced by active blind thrusts in the southern Abruzzi peri-Adriatic belt (Central Italy). Geogr. Fis. Din. Quat. 43, 3–13. https://doi.org/10.4461/GFDQ.2020.43.1.

Reimann, T., Tsukamoto, S., 2012. Dating the recent past (<500 years) by post-IR IRSL feldspar examples from the North Sea and Baltic Sea coast. Quat. Geochronol. 10, 180–187. https://doi.org/10.1016/j.quageo.2012.04.011.

Rose, J., 1995. Lateglacial and early Holocene river activity in lowland Britain. European river activity and climatic change during the Lateglacial and early. Holocene 14, 51–74.

Schanz, S.A., Montgomery, D.R., 2016. Lithologic controls on valley width and strath terrace formation. Geomorphology 258, 58–68. https://doi.org/10.1016/j.geomorph.2016.01.015.

Schanz, S.A., Montgomery, D.R., Collins, B.D., Duvall, A.R., 2018. Multiple paths to straths: a review and reassessment of terrace genesis. Geomorphology 312, 12–23. https://doi.org/10.1016/j.geomorph.2018.03.028.

Schumm, S.A., 1993. River response to baselevel change: implications for sequence stratigraphy. J. Geol. 101 (2), 279–294.

Schwanghart, W., Scherler, D., 2014. TopoToolbox 2–MATLAB-based software for topographic analysis and modeling in Earth surface sciences. Earth Surf. Dyn. 2 (1), 1–7. https://doi.org/10.5194/esurf-2-1-2014.

Selli, R., 1954. Il bacino del Metauro: descrizione geologica, risorse minerarie, idrogeologia. Museo geologico Giovanni Cappellini.

Selli, R., 1962. Il Paleogene nel quadro della geologia dell'Italia meridionale. Mem. Soc. Geol. It 3 (7).

Sembroni, A., Molin, P., Soligo, M., Tuccimei, P., Anzalone, E., Billi, A., Franchini, S., Rinaldi, M., Tarchini, L., 2020. The uplift of the Adriatic flank of the Apennines since the Middle Pleistocene: new insights from the Tronto River basin and the Acquasanta Terme Travertine (central Italy). Geomorphology 352, 106990. https://doi.org/10.1016/j.geomorph.2019.106990.

Stange, K.M., Van Balen, R.T., Kasse, C., Vandenberghe, J., Carcaillet, J., 2014. Linking morphology across the glaciofluvial interface: a 10Be supported chronology of glacier advances and terrace formation in the Garonne River, northern Pyrenees, France. Geomorphology 207, 71–95. https://doi.org/10.1016/j.geomorph.2013.10.028.

Stehman, S.V., 1997. Selecting and interpreting measures of thematic classification accuracy. Remote Sens. Environ. 62 (1), 77–89. https://doi.org/10.1016/S0034-4257(97)00083-7.

Storms, J.E., Weltje, G.J., Terra, G.J., Cattaneo, A., Trincardi, F., 2008. Coastal dynamics under conditions of rapid sea-level rise: Late Pleistocene to Early Holocene evolution of barrier–lagoon systems on the northern Adriatic shelf (Italy). Quat. Sci. Rev. 27 (11−12), 1107–1123. https://doi.org/10.1016/j.quascirev.2008.02.009.

Taddeucci, A., Tuccimei, P., Voltaggio, M., 1992. Studio geocronologico del complesso carsico "Grotta del Fiume-Grotta Grande del Vento" (Gola di Frasassi, Ancona) e implicazioni paleoambientali.

Trauerstein, M., Lowick, S.E., Preusser, F., Schlunegger, F., 2014. Small aliquot and single grain IRSL and post-IR IRSL dating of fluvial and alluvial sediments from the Pativilca valley, Peru. Quat. Geochronol. 22 (163–174), 1014–1871. https://doi.org/10.1016/j.quageo.2013.12.004.

Troiani, F., Della Seta, M., 2011. Geomorphological response of fluvial and coastal terraces to Quaternary tectonics and climate as revealed by geostatistical topographic analysis. Earth Surf. Process. Landf. 36 (9), 1193–1208. https://doi.org/10.1002/esp.2145.

Vandenberghe, J., 1995. Timescales, climate and river development. Quat. Sci. Rev. 14 (6), 631–638.

Villa, G.M., 1942. Nuove ricerche sui terrazzi fluviali delle Marche.

Viveen, W., Sanjurjo-Sanchez, J., Rosas, M.A., Vanacker, V., Villegas-Lanza, J.C., 2022. Heinrich events and tectonic uplift as possible drivers for late Quaternary fluvial dynamics in the western Peruvian Andes. Global Planet. Change 103972. https://doi.org/10.1016/j.gloplacha.2022.103972.

Wang, A., Smith, J.A., Wang, G., Zhang, K., Xiang, S., Liu, D., 2009. Late Quaternary river terrace sequences in the eastern Kunlun Range, northern Tibet: a combined record of climatic change and surface uplift. J. Asian Earth Sci. 34 (4), 532–543. https://doi.org/10.1016/j.jseaes.2008.09.003.

Wang, Q.L., Wang, J.H., Zhu, G.Z., Cui, D.X., Wang, W.P., Chen, Z.S., Song, Z.S., 2004. Vertical deformations of the eastern Kunlun fault zone and west of Kunlun Mountain pass Ms8. 1 earthquake. Seismol. Geol. 26 (2), 273–280.

Wegmann, K.W., Pazzaglia, F.J., 2002. Holocene strath terraces, climate change, and active tectonics: the Clearwater River basin, Olympic Peninsula, Washington State. Geol. Soc. Am. Bull. 114 (6), 731–744. https://doi.org/10.1130/0016-7606(2002)114%3C0731:HSTCCA%3E2.0.CO;2.

Wegmann, K.W., Pazzaglia, F.J., 2009. Late Quaternary fluvial terraces of the Romagna and Marche Apennines, Italy: Climatic, lithologic, and tectonic controls on terrace genesis in an active orogen. Quat. Sci. Rev. 28 (1–2), 137–165. https://doi.org/10.1016/j.quascirev.2008.10.006.

Westaway, R., Maddy, D., Bridgland, D., 2002. Flow in the lower continental crust as a mechanism for the Quaternary uplift of south-east England: constraints from the Thames terrace record. Quat. Sci. Rev. 21 (4–6), 559–603. https://doi.org/10.1016/S0277-3791(01)00040-3.

Wu, D., Li, B., Lu, H., Zhao, J., Zheng, X., Li, Y., 2020. Spatial variations of river incision rate in the northern Chinese Tian Shan range derived from late Quaternary fluvial terraces. Global Planet. Change 185, 103082. https://doi.org/10.1016/j.gloplacha.2019.103082.

Zepner, L., Karrasch, P., Wiemann, F., Bernard, L., 2021. ClimateCharts. Net–an interactive climate analysis web platform. Int. J. Digit. Earth 14 (3), 338–356. https://doi.org/10.1080/17538947.2020.1829112.

Zhang, J.Y., Liu-Zeng, J., Scherler, D., Yin, A., Wang, W., Tang, M.Y., Li, Z.F., 2018. Spatiotemporal variation of late Quaternary river incision rates in Southeast Tibet, constrained by dating fluvial terraces. Lithosphere 10 (5), 662–675. https://doi.org/10.1130/L686.1.

Zondervan, J.R., Stokes, M., Telfer, M.W., Boulton, S.J., Mather, A.E., Buylaert, J.P., Belfoul, M.A., 2022. Constraining a model of punctuated river incision for Quaternary strath terrace formation. Geomorphology 414, 108396. https://doi.org/10.1016/j.geomorph.2022.108396.